



D25: Lake stratification studies

Work package No. 4:	Lake stratification
Lead contractor:	HYD
Main objective:	Key processes
Strategic leader:	Dr. Loga-Karpinska (WUT)
Responsible task leader:	Dr. Baumert (HYD)

Main contributors involved:	Organisation	E-Mail
Helmut Baumert	HYD	Baumert@hydromod.de
Kurt Duwe	HYD	Duwe@hydromod.de
Semen Levikov	HYD	Levikov@hydromod.de
Victor Podsetchine	PRC	victor.podsetchine@vyh.fi
Anu Peltonen	PRC	anu.peltonen@vyh.fi
Malgorzata Loga-Karpinska	WUT	Malgorzata.loga@is.pw.edu.pl
Maciej Filocha	WUT	maciej.filocha@is.pw.edu.pl
Ulrich Lemmin	EPF	ulrich.lemmin@epfl.ch
Dominique Fontvieille	CAR	dfont@univ-savoie.fr
Patrick Sauvaget	SOG	patrick.sauvaget@sogreah.fr
Claude Guilbaud	SOG	claud.guilbaud@sogreah.fr
Matthew O'Hare	UoG	mohare@geog.gla.ac.uk
Kevin Murphy	UoG	k.murphy@bio.gla.ac.uk
Jane Drummond	UoG	j.drummond@geog.gla.ac.uk
Colin Adams	UoG	c.adams@bio.gla.ac.uk
Eckard Hollan	ISF	eckard.hollan@lfula.lfu.bwl.de
Hans Güde	ISF	hans.guede@lfula.lfu.bwl.de
Bernd Wahl	ISF	isf.eurolakes@lfula.lfu.bwl.de

Dissemination level: Public

Table of Contents

1	Executive Summary	3
2	Introduction	6
3	Part I: Warsaw University of Technology	7
3.1	BRIEF CHARACTERISATION OF STUDY SITE	7
3.2	THE MODEL	8
3.3	SIMULATIONS	9
3.4	SUMMARY	11
3.4.1	<i>General</i>	11
3.4.2	<i>Particular</i>	11
4	Part II: Pirkanmaa Regional Environment Centre.....	13
4.1	INTRODUCTION AND OBJECTIVES.....	13
4.2	APPLICATION TO LOCH LOMOND.....	13
4.2.1	<i>Brief site description</i>	13
4.2.2	<i>Calibration</i>	14
4.3	APPLICATION TO BOURGET LAKE	18
4.3.1	<i>Brief site description</i>	18
4.3.2	<i>Calibration</i>	18
4.4	APPLICATION TO LAKE LÄNGELMÄVESI-ROINE.....	20
4.4.1	<i>General description of the application</i>	20
4.4.2	<i>Calibration</i>	20
5	PART III: SOGREAH	22
5.1	INTRODUCTION	22
5.2	BOURGET LAKE VERSUS UPPER LAKE CONSTANCE.....	25
5.3	CONCLUSIONS	27
6	Part IV: Ecole Polytechnique Federale Lausanne	28
6.1	INTRODUCTION	28
6.2	LAKE STRATIFICATION DYNAMICS.....	28
6.3	THERMOCLINE DEPTH	31
6.4	MIXING DYNAMICS	33
6.5	LONGTERM TRENDS	38
6.6	CONCLUSIONS.....	40
7	Part V: HYDROMOD Scientific Consulting.....	43
7.1	OVERVIEW	43
7.2	SELECTED RESULTS	45
7.3	APPLICATION TO LAKE GENEVA.....	50
7.4	CONCLUSIONS.....	52

References

1 EXECUTIVE SUMMARY

This report summarises results achieved and research activities made in EURLAKES WorkPackage 04 on Stratification. The report begins with a brief account on a 3D modelling effort by WUT using the hydro-thermodynamic FEM code TELEMAC-3D for simulating Bourget Lake which covers simulation times of some hundred hours with high horizontal and intermediate vertical resolution (18 layers). Based on an observed phase shift between the measured and modelled long internal waves (seiches) it is concluded that some internal-seiche features are not described satisfactorily. As the major candidate reason inadequate calibration of the model parameters is identified.

The report is continued by PRC with a series of model calibration studies for long-term applications of the PROBE model. The latter has originally been elaborated by Svensson about 18 years ago and improved by PRC scientists since the early 90th. It is a 1D water-column model with high vertical resolution, here with up to 140 layers of about 1 meter thickness each. The individual calibrations of the model for Loch Lomond, Lake Längelmävesi-Roine and Bourget Lake demonstrate the substantial overall predictive capability of the code although in the case of Bourget Lake the thermal reaction appears with a minor delay of some days. This is not the case for the other lakes under study. As a major problem for the evaluation of the quality of the code appears the lack of adequate reference observations of critical state variables of the model. This is a general problem for almost all deep large lakes and corresponding models (The same applies to the HYDROMOD model LAKE1D). We recommend to include fortnightly profiles of conductivity, temperature, turbidity and fluorescence (if possible: plus major ions) in the routine monitoring programmes of those lakes, where not already done. A major point here is stability of the measurement technology over years to allow inter-decadal comparisons for the detection of climate-change and long-term anthropogenic (land-use change etc.) signals mainly in the deeper parts of the lakes under consideration.

The latter point is picked up in the contribution by SOGREAH which concentrates on a comparative study of the long-term evolution of deep-water temperatures in Lake Constance and Bourget Lake. This brief but instructive study shows that both lakes belong to the same climate region as their deep-water temperatures exhibit almost synchronicity and a high intercorrelation (with a long-term mean temperature difference at the deepest points of about 1.5°C). Although Lake Constance is 100 meters deeper than Bourget Lake and located about 170 meters higher above sea level, in the period 1986 to 2001 both lakes behave very similarly not only with respect to their deep-water temperature but also – though less pronounced – with respect to their deep-water ventilation (oxygen concentration). This study underlines the strong correlation between hydro-thermodynamic effects like winterly deep-water renewal and deep-water ventilation (re-oxygenation) of the hypolimnion. This is of paramount importance for the prediction of the health of deep large lakes.

The part which follows is a contribution by EPFL who studied Lake Geneva with respect to the interplay between stratification and mixing, with a focus on basin-wide and long-term results. The reported results are highly instructive and internationally unique as it is the only known case in which a large deep lake is characterised by careful observations of mixing characteristics. We notice that an intercomparison between the long-

term trends in Lake Geneva with the a.m. correlations between Lake Constance and Bourget Lake has not yet been carried out but would be worth to concentrate forces on this highly relevant issue in the future.

In the last contribution to this EUROLAKES Deliverable D25, HYDROMOD concentrates on more fundamental physical aspects of stratification modelling where it rests on dedicated laboratory studies under idealised conditions rather than on field research, e.g. on the neutrally buoyant wave-enhanced surface layer, the Monin-Obukhov problem in the upper parts of the epilimnion, and on laboratory studies of the collapse of turbulence into internal waves and the behaviour of various turbulence scales under shear and stratification. Using only a few equations, in the present Report the central features of the new theoretical closure are confronted graphically with the dedicated measurements mentioned above. Interestingly, the new closure is free of empirical parameters. The application of the closure reported here is twofold: (i) in long-term climate and management scenario simulations as documented in the EUROLAKES Deliverable D20 belonging to EUROLAKES Workpackage 22; (ii) in an intercomparison with the results achieved by EPFL for Lake Geneva. This latter intercomparison shows a basically well agreement between the theoretical closure and the observations in this deep large lake. For the interested reader further theoretical details of the new closure are presented in ANNEX A to the present report.

Table of Contents



	1	1
1	Executive Summary	3
2	Introduction	6
3	Part I: Warsaw university of technology	7
3.1	BRIEF CHARACTERIZATION OF STUDY SITE	7
3.2	THE MODEL	8
3.3	SIMULATIONS	9
3.4	SUMMARY	11
3.4.1	<i>General</i>	11
3.4.2	<i>Particular</i>	11
4	Part II: Pirkanmaa Regional Environment Centre	13
4.1	INTRODUCTION AND OBJECTIVES	13
4.2	APPLICATION TO LOCH LOMOND	13
4.2.1	<i>Brief site description</i>	13
4.2.2	<i>Calibration</i>	14
4.3	APPLICATION TO BOURGET LAKE	18
4.3.1	<i>Brief site description</i>	18
4.3.2	<i>Calibration</i>	18
4.4	APPLICATION TO LAKE LÄNGELMÄVESI-ROINE	20
4.4.1	<i>General description of the application</i>	20
4.4.2	<i>Calibration</i>	20
5	PART III: SOGREAH	22
5.1	INTRODUCTION	22
5.2	BOURGET LAKE VERSUS UPPER LAKE CONSTANCE	25
5.3	CONCLUSIONS	27
	Part IV: Ecole Polytechnique federale Lausanne	28
5.4	INTRODUCTION	28
5.5	LAKE STRATIFICATION DYNAMICS	28
5.6	THERMOCLINE DEPTH	31
5.7	MIXING DYNAMICS	33
5.8	LONGTERM TRENDS	38
5.9	CONCLUSIONS	40
6	Part V: HYDROMOD Scientific Consulting	43
6.1	OVERVIEW	43
6.2	SELECTED RESULTS	45
6.3	APPLICATION TO LAKE GENEVA	50
6.4	CONCLUSIONS	52
7	list of references	53

2 INTRODUCTION

The formation and break-up or erosion of stratification is a major process in all natural and man-made lakes which controls to a large extent the health of their ecosystems. Since long the correct description of limnologically relevant lake states like “full circulation” or “summer stagnation” etc. are challenging researchers from various fields, from applied researchers and observationalists in limnology, lake physics, reservoir ecology and oceanography to theoretical and mathematical physics. The key challenge here is the specific role of shear generated and convective turbulence in the formation/destruction of stratification and their interactions with internal waves.

In contrast to other fields of physics, all problems which are significantly governed by turbulence are today still poorly understood due to our lack of understanding of the nature and behaviour of the proper turbulence. It remains as **the** last unresolved problem of classical physics of the last 75 years. This situation should be kept in mind when evaluating any progress in understanding lake stratification.

Another point is the observational problem. While it is relatively easy to measure vertical temperature profiles in deep lakes using devices like the famous classical high-precision bathysonde (later on called CTD probe) or thermistor chains, the data gained that way are still only footprints of the acting physical turbulence and mixing processes. The direct measurement of the latter is difficult. Moreover, field measurements in lakes are mostly made when nearly all possible lake processes are in action so that it is extremely difficult to single out specific processes and their cause-effect relationships.

Fortunately, today devices like ADCP or free-falling profilers like the SST probe are available which measure relevant fine- and micro-scales of the turbulence proper, e.g. the so-called Thorpe scale and the Ozmidov scale. Although specific measurement campaigns with those probes were/are not part of the EUROLAKES project, some partners could contribute their experience from other projects to the EUROLAKES Work-Package 04 on stratification. Further, today we may rest on a set of solid laboratory experiments which represent serious and critical test cases which should be satisfied by any turbulence model or ‘scheme’ before it is applied to field data of real-world lakes. In other words, although lake stratification remains a fundamental challenge, the situation improved within the last 10 to 20 years significantly. The following contributions rest essentially on those progresses gained in other fields.

3 PART I: WARSAW UNIVERSITY OF TECHNOLOGY

Stratification modelling for Bourget Lake¹

3.1 BRIEF CHARACTERISATION OF STUDY SITE

Bourget Lake is the largest natural lake in France (Area: 44.5 km²). It is a narrow lake situated in Savoy (Length: 18 km; Width: 1.6 km at Saint-Innocent point, 3.2 km at Grésine). The lake is set in a syncline at the foot of the alpine mountain (Average depth: 85 m; maximum depth: 145 m). The mean lake surface altitude is 231 m.

The rivers Leysse and Sierroz are the two main tributaries recharging the lake. The Savières channel, connected to the Rhône river, is the main outflow. A sketch of the lake and the main rivers is shown in Figure 1.

The annual mean flow of the Leysse river is about 8.5 m³/s with a peak of average 100 m³/s during flood events. The annual mean flow of the Sierroz river is about 3.5 m³/s and the flow reaches 30 m³/s during flood events.

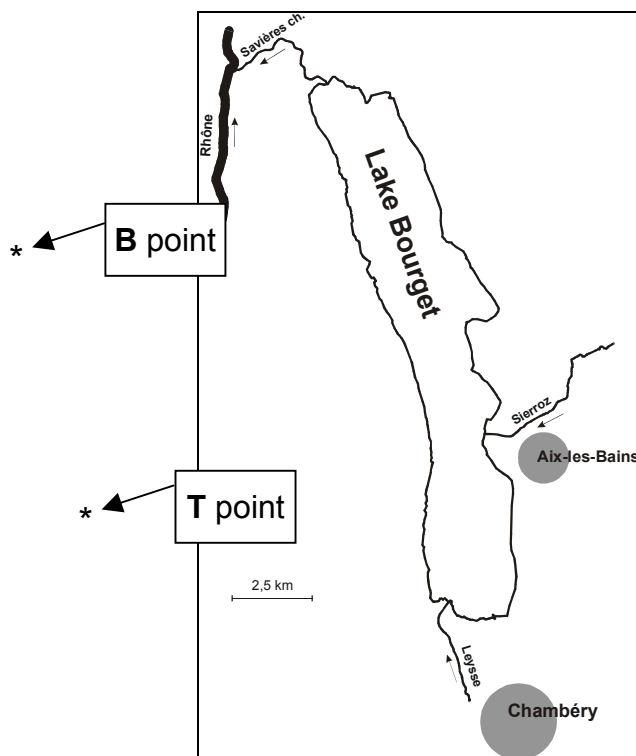


Figure 3-1 Schematic view of the lake

Lake stratification analysis was based on the only data available during the Eurolakes project – 50 measurements campaigns made during the period between 12 January 1994 and 17 December 1996 in the deepest part of the lake. In that point (marked as

¹ Authors of PART I:
Maciej Filocha from WUT

“B” on the Figure 1) roughly every two weeks thermal profiles has been sounded. A simple time-depth interpolation of these data is plotted in the Figure 2.

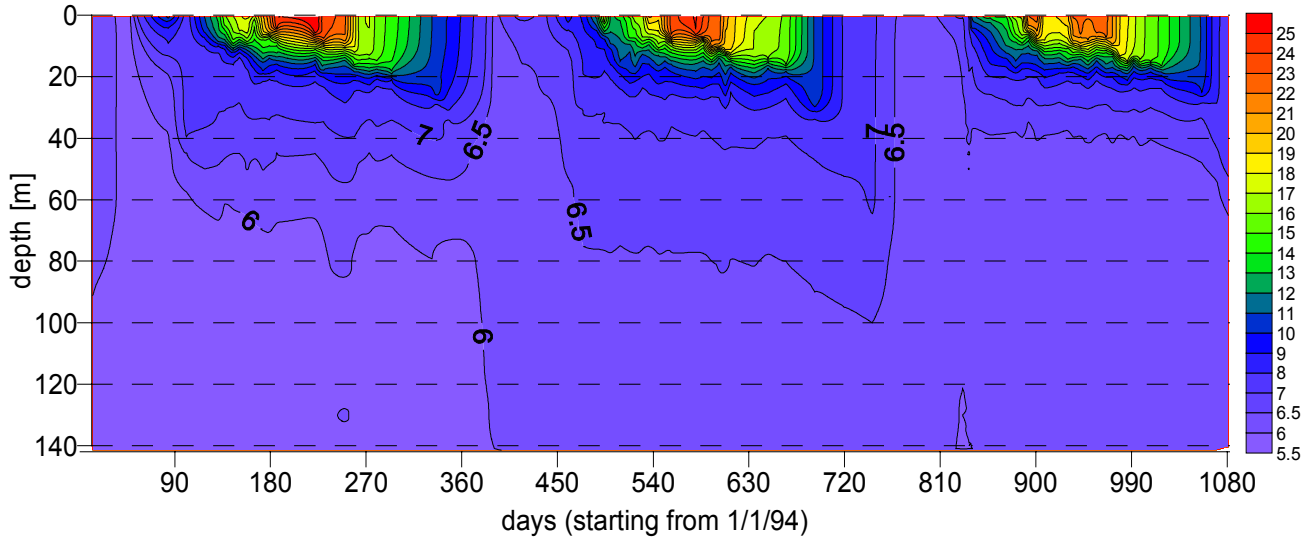


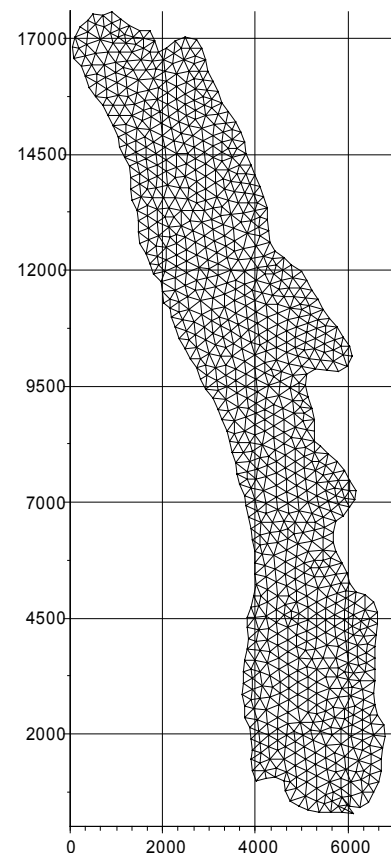
Figure 3-2 Thermal profiles in the "B" point

3.2 THE MODEL

A three dimensional numerical model of the lake was built using the TELEMAC-3D software. The finite element software TELEMAC-3D solves the Navier-Stokes equation with a free surface boundary condition and the advection-diffusion equations for temperature and other active or passive scalar variables [Janin et al., 1992]. Density effects, wind stress on the free surface and the Coriolis force are included in the model. Variations of the density are taken into account in the momentum equations via Boussinesq approximation.

Computational mesh consists of approximately 17000 nodes, formed in 30000 prisms and grouped in 18 horizontal layers. A plane and 3D isometric views of the mesh are shown in Figures 3 and 4.

Figure 3-3
 Finite element mesh – plane view
 (coordinates in meters)



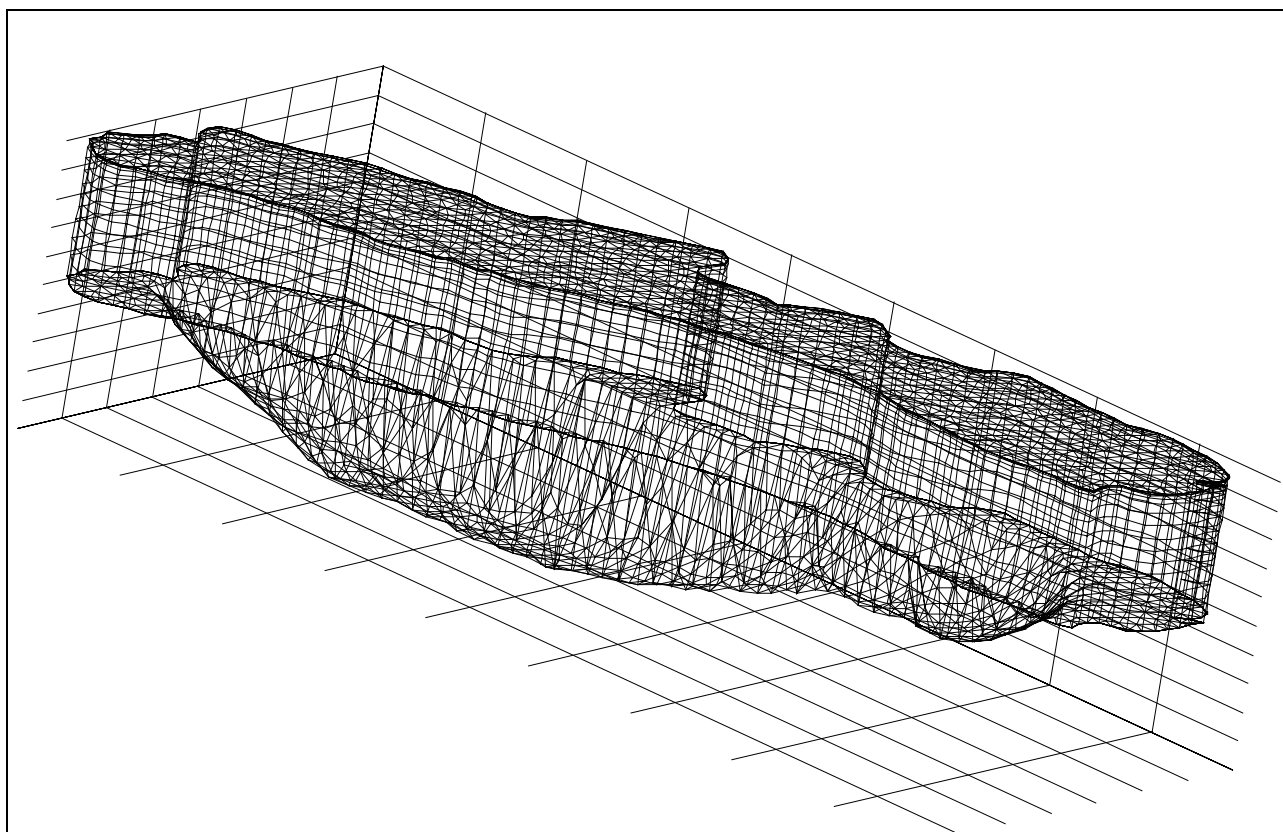
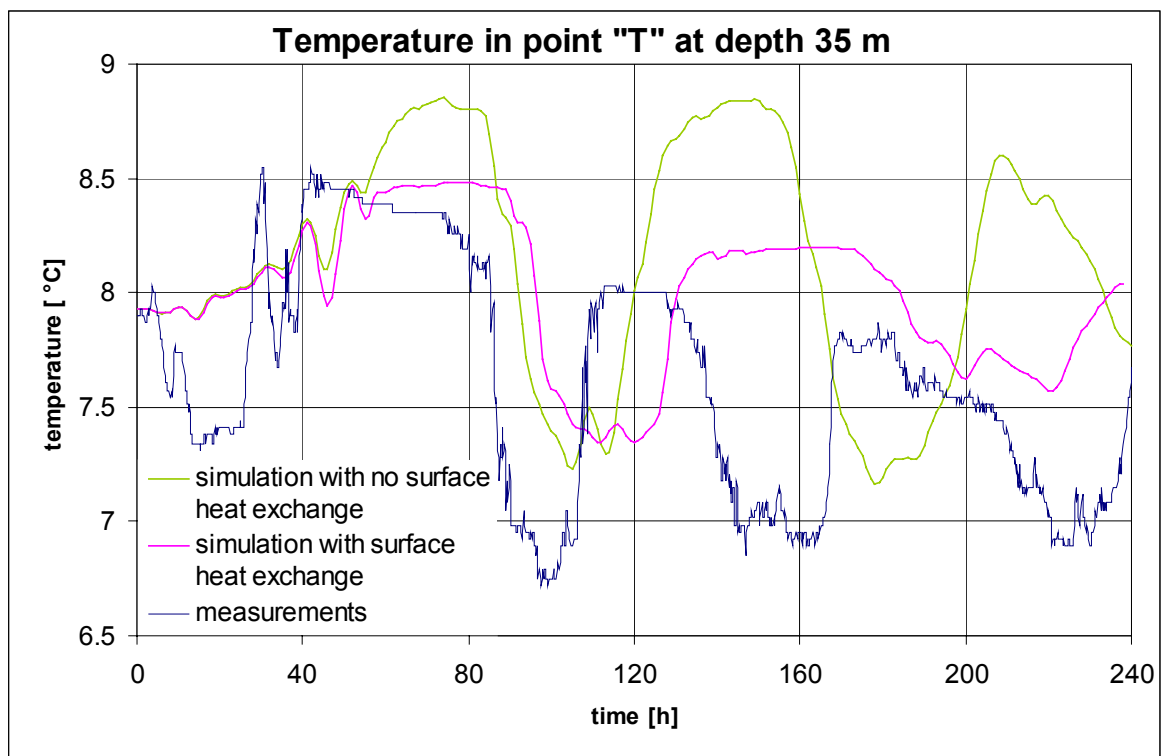
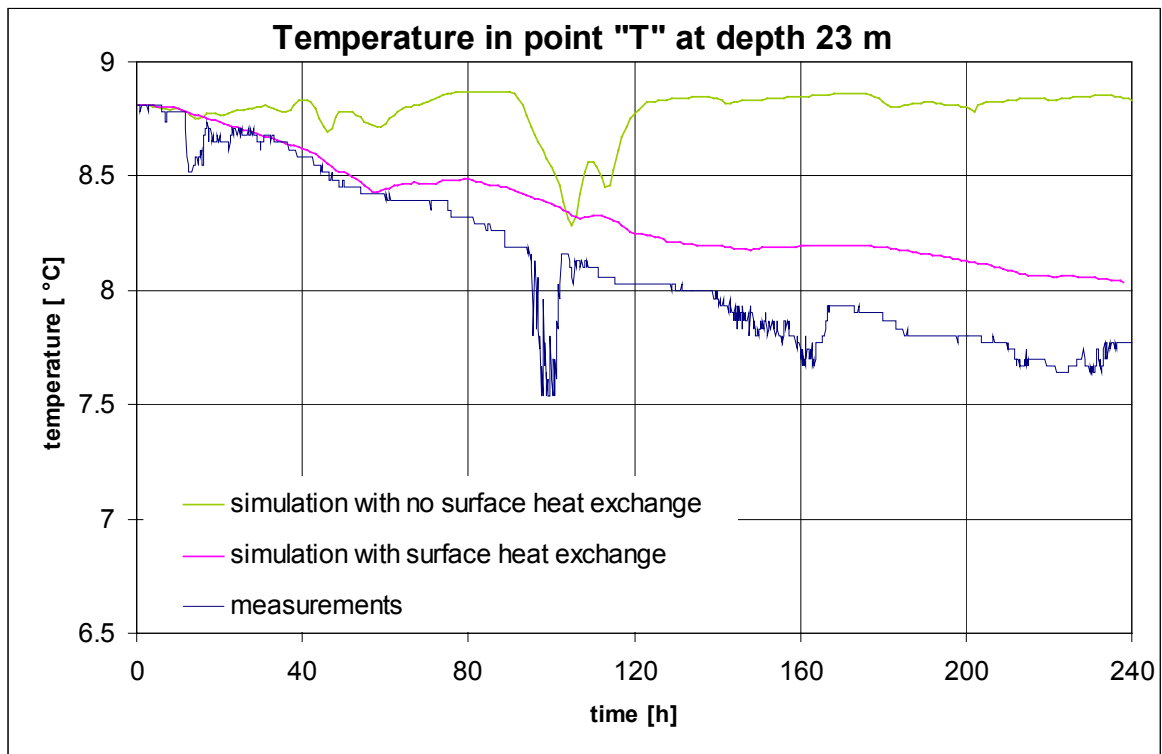


Figure 3-4 A 3D view of the computational mesh

3.3 SIMULATIONS

Selected scenarios of thermal stratification and wind action have been simulated in TELEMAC-3D. Also, an energy exchange through the water surface term (long- and short-wave radiation) has been tested. In the example below, a comparison between collected data and computed results in point "T" is shown. For that simulation, winter period of 10 days, starting 11 December 1995 has been chosen. Real wind data recorded by meteorological station located on the lake bank and then extrapolated over all lake area was used.

Surface heat exchange module allowed for reconstructing general descending trend of the temperature for different water depths. However, there are still problems of underestimating cooling effect and attenuating of internal waves especially in the upper layers (see fig 5a) of the model.



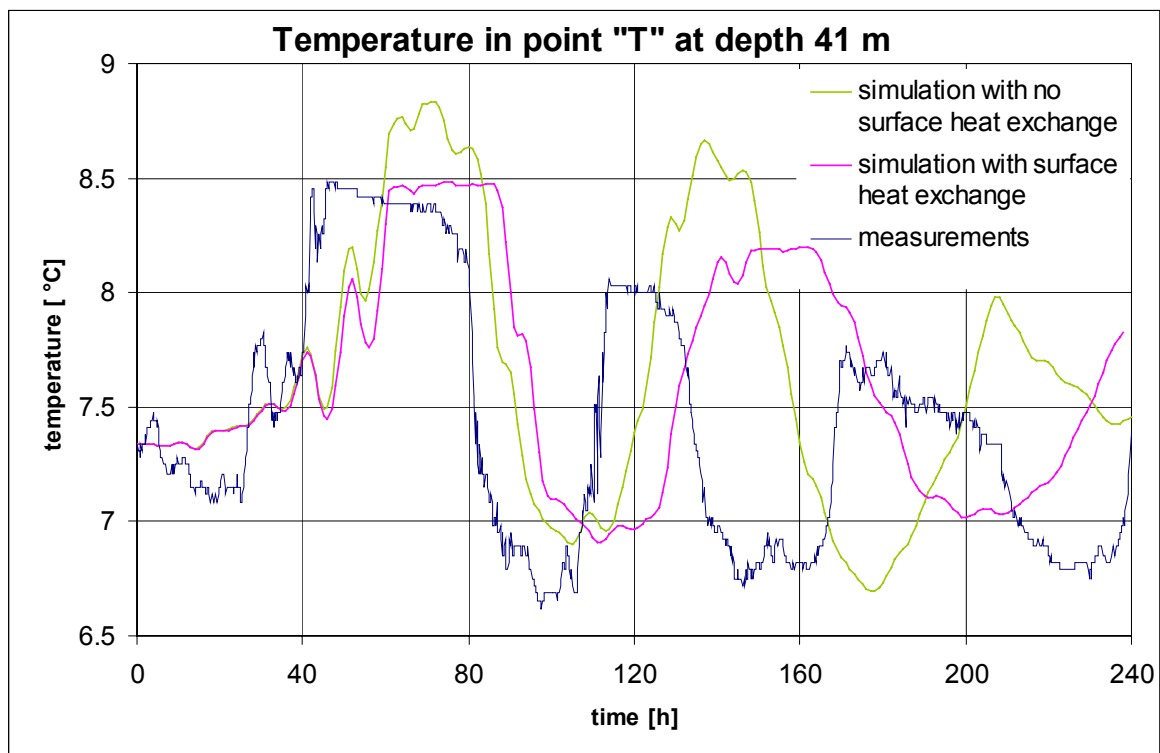


Figure 3-5 (a, b, c) Comparison between measured data and simulated results in selected point

3.4 SUMMARY

3.4.1 General

A computational power of modern computers allows us to use one-dimensional models that couples laterally-averaged lake physics and water quality modelling to examine long-term sensitivity to anthropogenic changes in the catchment or fluctuations in local climate. Such approach for predicting evolution of lake stratification and water quality over 50 or 100-year periods will be dominant for the near future [Imberger et al. 2000]. On the other hand, transport processes in lake, which are of the most importance for biochemical cycle, are inherently three-dimensional. Having in mind computational and memory constrains that restrict our modelling horizon to weekly to monthly simulations it is good to know that modelling in 3D provides better resolution of topographical effects, internal waves, mixing and spatial gradients of environmental forcing. Hence, it can be envisaged that, parallel to 1D vertical modelling, the 3D modelling of lake stratification (that takes into account these effects) will be attempted possibly following new developments in computer technologies. At the same time new field experiments and continuous observations will be executed to refine our understanding of the lake physics and biological processes running in lakes. These two trends will meet one day resulting in 3D computer simulations of inherently 3D reality of the lake processes.

3.4.2 Particular

As the result of simulations of the Bourget Lake stratification using the TELEMAC-3D model the following effects have been reconstructed quite satisfactory for the selected (short) period of time:

- Internal waves show reasonable similarity to the observed waves in terms of time-changes of water temperature at some fixed point and different depths of the lake.
- “Activating” energy exchange term at the surface of the lake allowed for reconstructing general descending trend of the temperature for different water depths.

However, a phase shift between the observed and modelled internal waves indicates that some effects are not reconstructed satisfactorily. The result of the shift can be caused, for instance, by inadequate calibration of the model parameters. Attempts of improving this aspect of modelling will be continued. As mentioned above also long-term simulations of the lake stratification have proven to be infeasible, mainly due to long computing time.

It should be mentioned also that a class of so-called “three-dimensional shallow water models” based on the finite element mesh space discretization, like TELEMAC-3D for example, often suffers from widely used method of σ -transformation. This method allows programmers to extent their 2D code into 3rd dimension and users to build easily 3D computational mesh based on simpler 2D horizontal mesh as well. However, the simplification can cause instabilities when solving numerically very sensible density transport effects. In lake modelling these transport mechanisms are usually much more important than inflow and outflow dynamic forcing.

It can be envisaged that full 3D finite element meshes can reproduce spatially arbitrary chosen regions of interest in the lake much better and hence allow for higher accuracy and numerical stability.

4 PART II: PIRKANMAA REGIONAL ENVIRONMENT CENTRE

Calculation of lake stratification²

4.1 INTRODUCTION AND OBJECTIVES

Water temperature and especially changes of temperature with depth is one of the most important physical, chemical and biological indicators of lake water quality. The annual cycle of stratification variability is determined by geographical location of the lake, morphological, hydrological features and meteorological factors.

The objective of this work package is stratification studies of lakes under study. The results of this work will provide quantitative information to be used in other work packages, especially in WP9 (Key processes). Here we mainly describe the modelling approach and calibration results for the three sites under consideration. Applied long-term studies are presented in the Final Report to EUROLAKES WorkPackage 22.

4.2 APPLICATION TO LOCH LOMOND

4.2.1 Brief site description

High-resolution non-steady one-dimensional model PROBE originally developed in Sweden (*Svensson*, 1986) and later extended in Finland (Malve et al., 1991, Frisk et al., 1997) was applied to all study lakes. The model neglects all gradients in horizontal direction. It solves momentum equations, heat energy, salinity and concentration equations. The vertical mixing is parameterised with k- ϵ model. The dynamic eddy viscosity is calculated from turbulence kinetic energy and dissipation rate with Prandtl-Kolmogorov relation. The meteorological forcing, water inflow and material fluxes are used to drive the model. Further details on numerical scheme and other technical details can be found in *Svensson* (1986) and Deliverable D13 (Work package 17).

The model applications differ from site to site depending on specific features of lakes and availability of input meteorological data.

Due to clear morphological differences Loch Lomond was divided into three separate sub-basins: shallow south part, mid basin and deep north basin (Fig. 4.1). The isolated versions of the model with constant grid cell size of 1 m were used. The cloudiness was estimated using measured solar radiation data.

²Authors of PART III:

Dr. *Tom Frisk* and Dr. *Victor Podsechine*

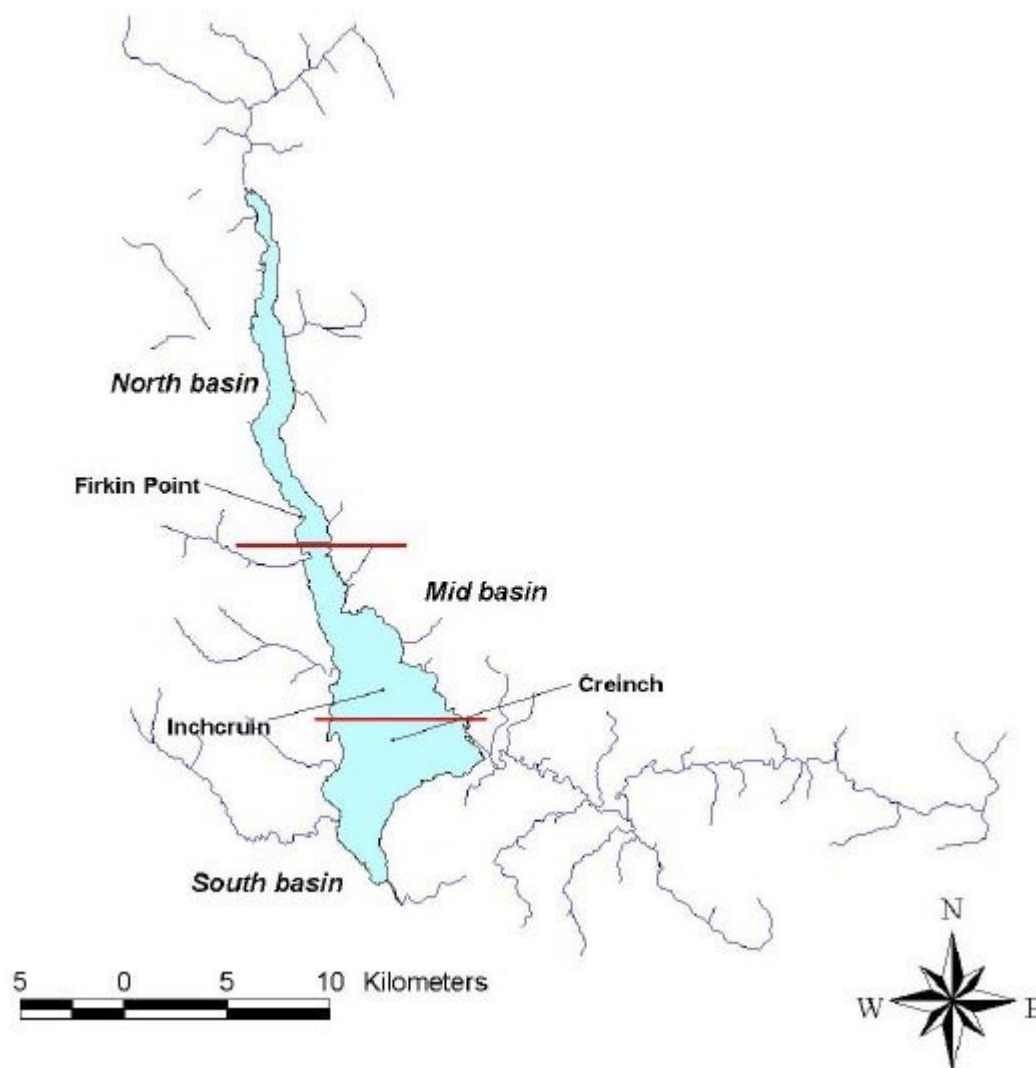


Fig. 4.1. Loch Lomond and observation sites used in calibration of the PROBE model.

4.2.2 Calibration

The model was calibrated against measured data for the three-year period from April 1989 till December 1992. The agreement between simulated results and observed data was good for all basins in the case of surface water temperature (Figs. 4.2, 4.4 and 4.6). Hydromod and University of Glasgow measured vertical profiles in summer 2001. They are plotted against calculated vertical distribution of water temperature for same dates in figures 4.3, 4.5 and 4.7. They cannot be compared directly due to differences in weather conditions but altogether they give an impression about possible range of temperature fluctuations in hypolimnion.

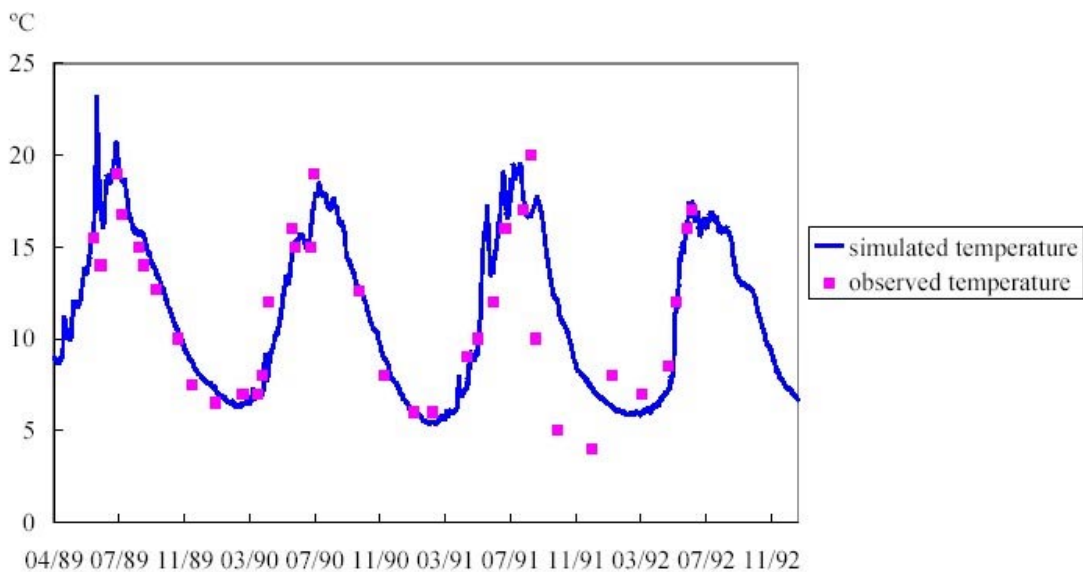


Fig. 4.2. Loch Lomond north basin, simulated and observed (Firkin Point) water temperature at the surface in 1989-1992.

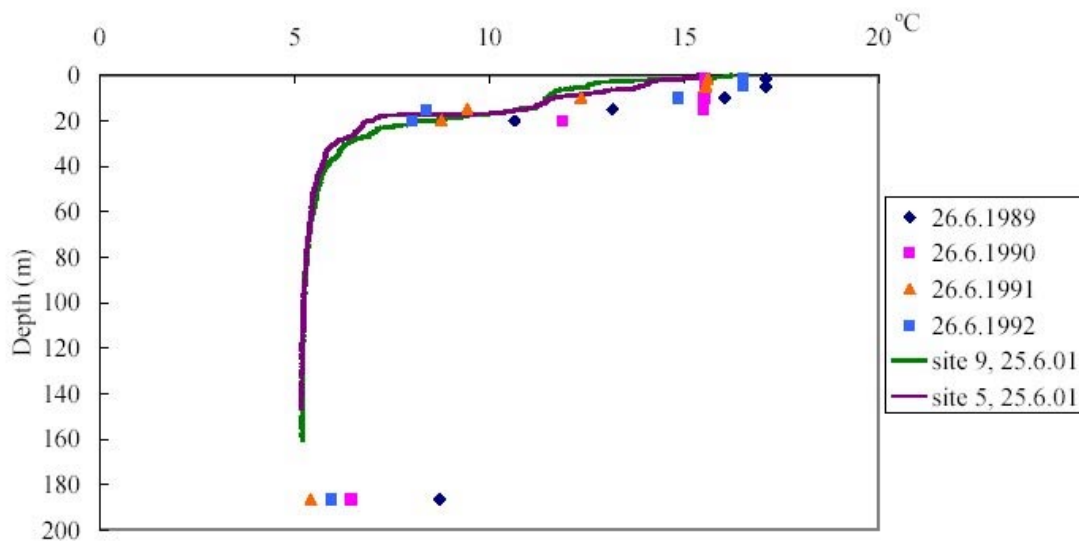


Fig. 4.3. Loch Lomond north basin, calculated and observed temperature profiles in June.

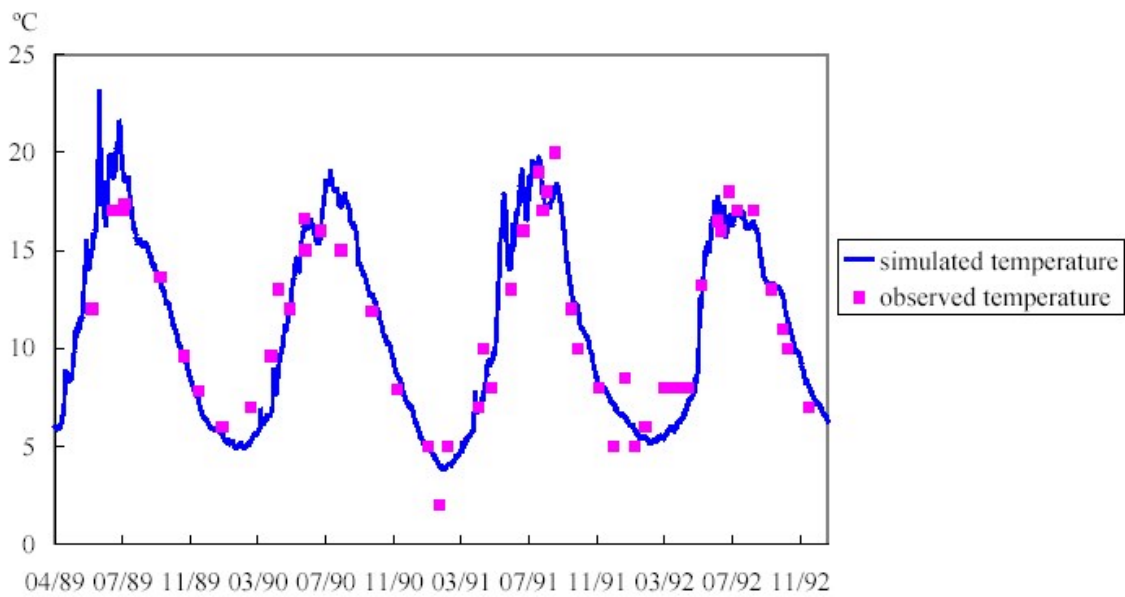


Fig. 4.4. Loch Lomond mid basin, simulated and observed (Inchcruin) water temperature at the surface in 1989-1992.

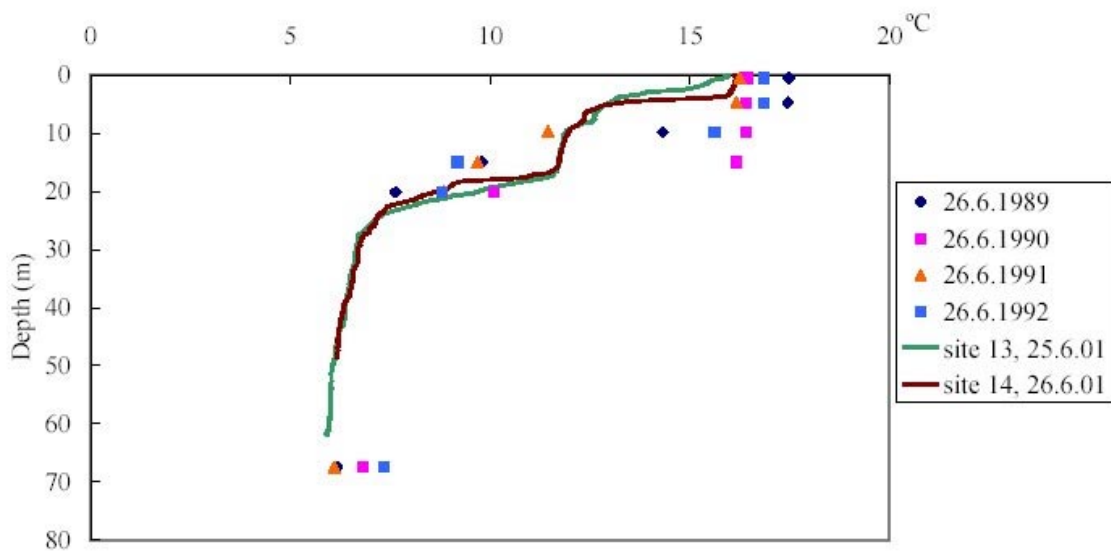


Fig. 4.5. Loch Lomond mid basin, calculated and observed temperature profiles in June.

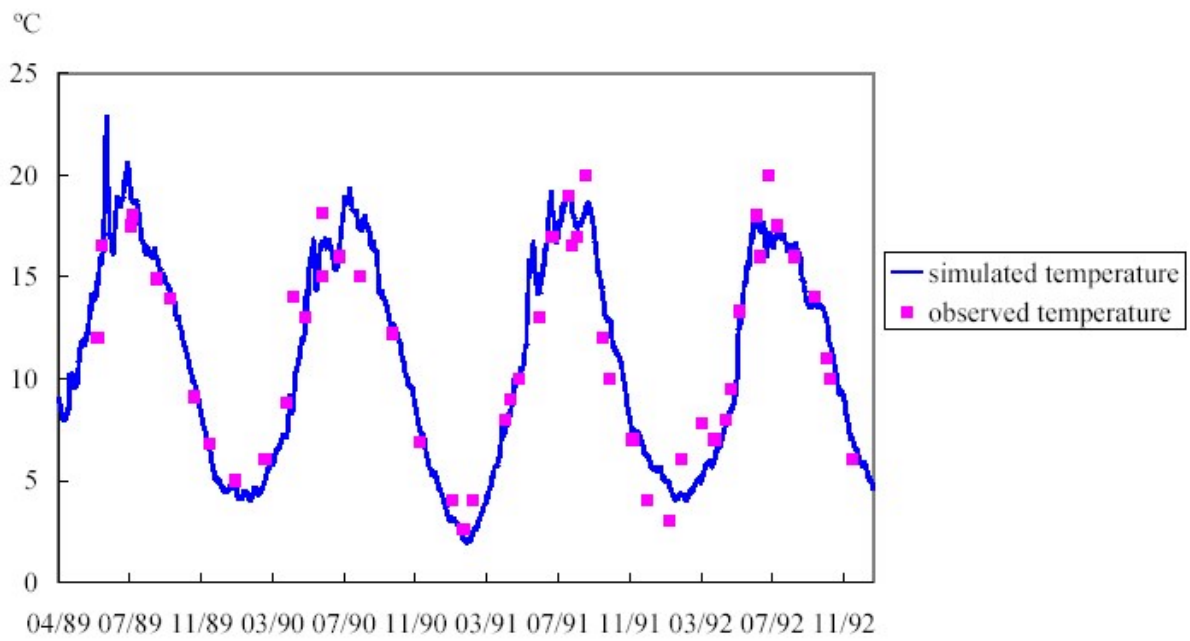


Fig. 4.6. Loch Lomond south basin, simulated and observed (Creinch) water temperature at the surface in 1989-1992.

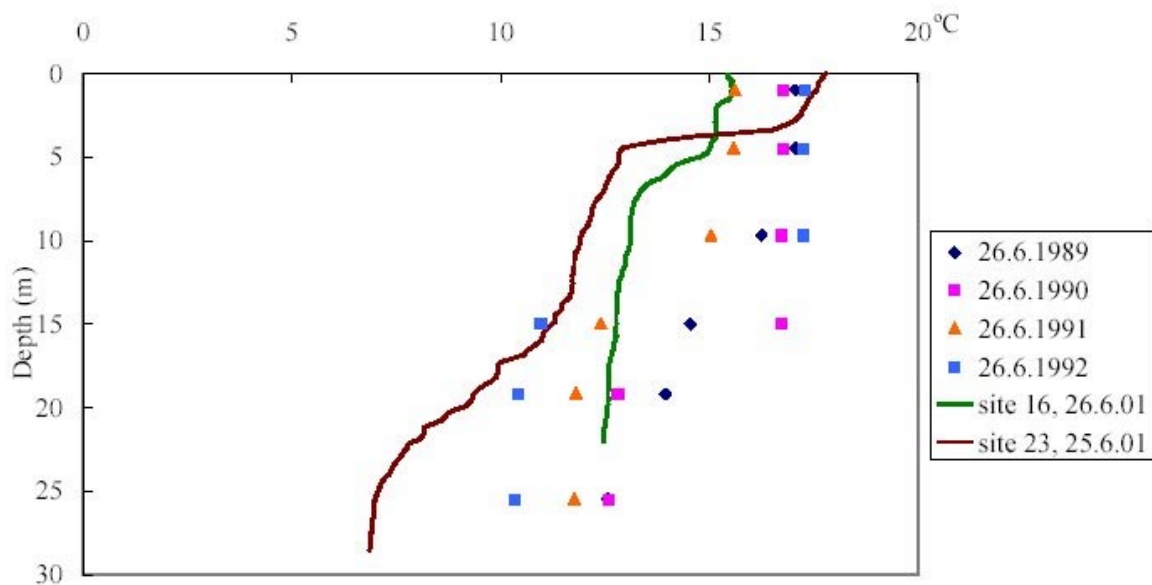


Fig. 4.7. Loch Lomond south basin, calculated and observed temperature profiles in June.

4.3 APPLICATION TO BOURGET LAKE

4.3.1 Brief site description

Due to simple morphology of Bourget Lake the one basin version of PROBE was applied. The vertical grid size was constant and equal to 1 m with total number of vertical layers of 140.

4.3.2 Calibration

The calibration period was from April 1994 till December 1995. As meteorological input the data from Voglans meteorostation located at the south shore of Bourget Lake were used. The data on cloudiness were not available and like in case of Loch Lomond they were approximated using observations on solar radiation and duration of daily light hours.

Figure 4.8 shows simulated and measured water temperature in the deepest point of the lake at different layers. The bottom temperature exceeds 5°C for the whole period. There is a clear phase shift in simulated surface temperature compared with observed ones.

These differences can be explained by the limitations of the one-dimensional approach. It should be kept in mind also that observations represent point measurements whereas the model reproduces lake or basin horizontally integrated vertical profiles. Vertical profiles for certain dates in summer 1994 and 1995 show good match between simulations and measurements (Fig. 4.9).

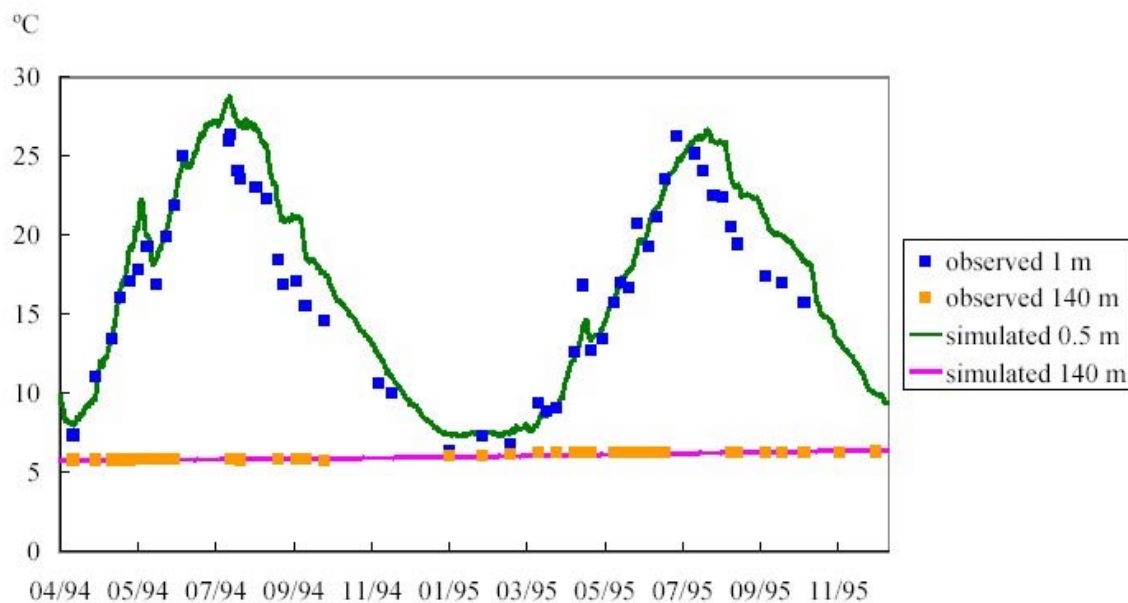


Figure 4-8 Bourget Lake, simulated and observed (site B) water temperature at the surface in 1994-1995.

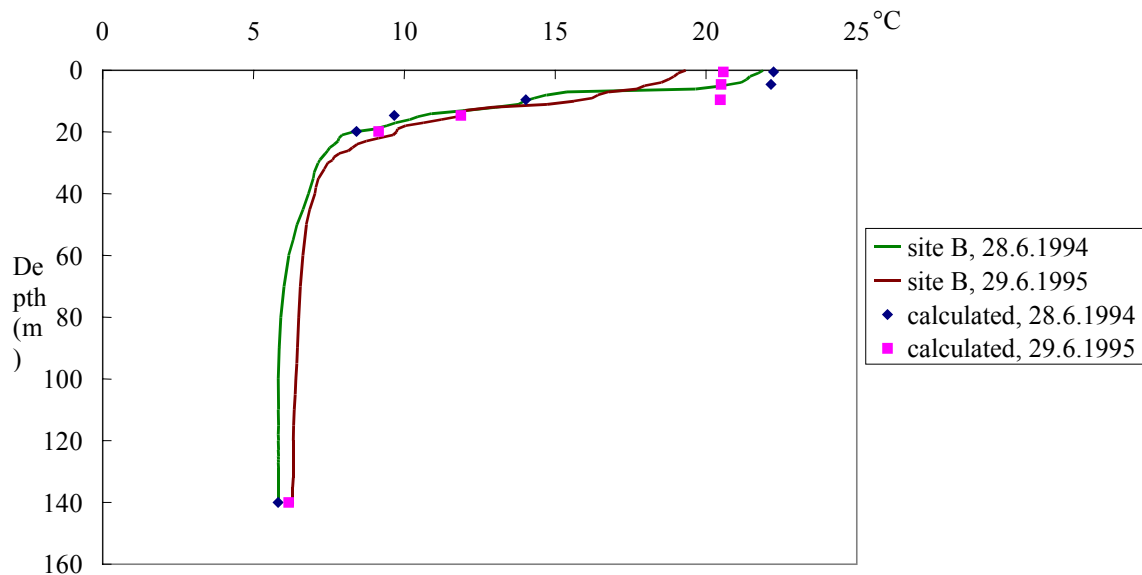


Figure 4-9 Bourget Lake, calculated and observed temperature profiles in June.

4.4 APPLICATION TO LAKE LÄNGELMÄVESI-ROINE

4.4.1 General description of the application

The one basin version of PROBE was applied to Lake Längelmävesi-Roine. The vertical grid size was constant and equal to 1 m with total number of vertical layers of 28.

4.4.2 Calibration

The calibration period was from April 2000 till December 2001. As meteorological input the data from Pirkkala airport were used.

Figure 4.10 shows simulated and measured water temperature in the deepest point of the lake at the surface and at the bottom. The simulated temperatures match the observed ones quite well at the surface but at the bottom simulated temperatures are too low. The same result can be seen in Fig. 4.9. which shows vertical profiles in August 2001.

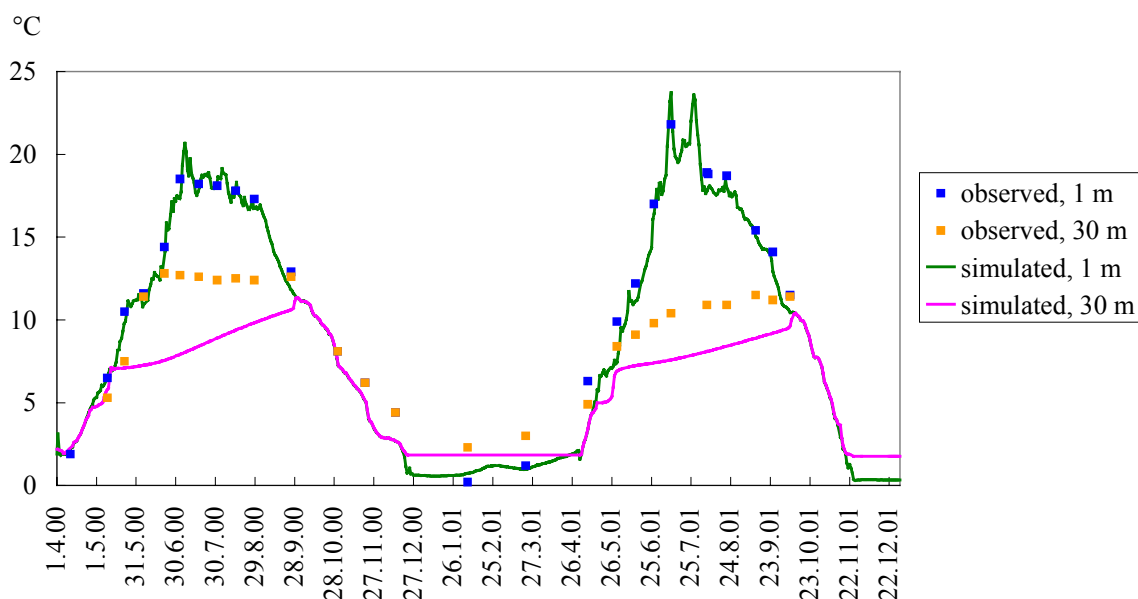


Fig. 4.10. Lake Roine, simulated and observed water temperature at the surface and at the bottom in 2000-2001.

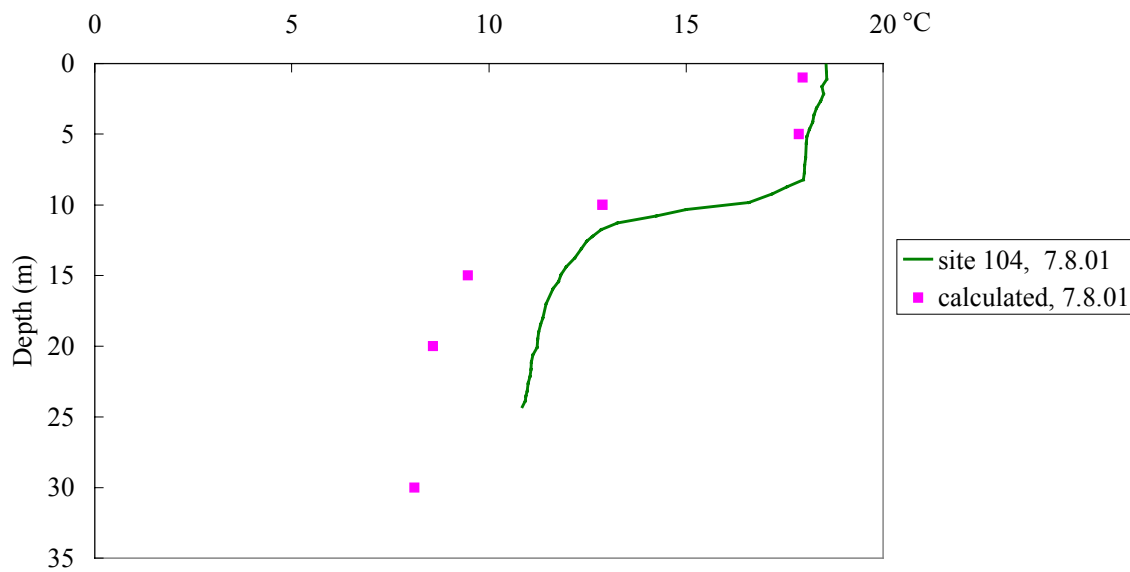


Fig. 4.11. Lake Roine, calculated and observed temperature profiles in August.

5 PART III: SOGREAH

Deep-water Temperature and oxygen concentration in Bourget Lake³

5.1 INTRODUCTION

The analysis of the deep temperature and oxygen are made on the measurement in the deeper part of the Bourget Lake at -130.0 m depth. Measurements on the Bourget Lake were provided by *La cellule technique du Bourget Lake* (France). Measurements in the lake Constance were provided by *Institut fuer Seenforschung* (Germany).

On the Figure 5.1, we present the time series of the temperature (°C) and the oxygen (mg/l) between 1986 and 2001. At the top of this figure, the lake frost days⁴ per winter seasons are presented (in blue).

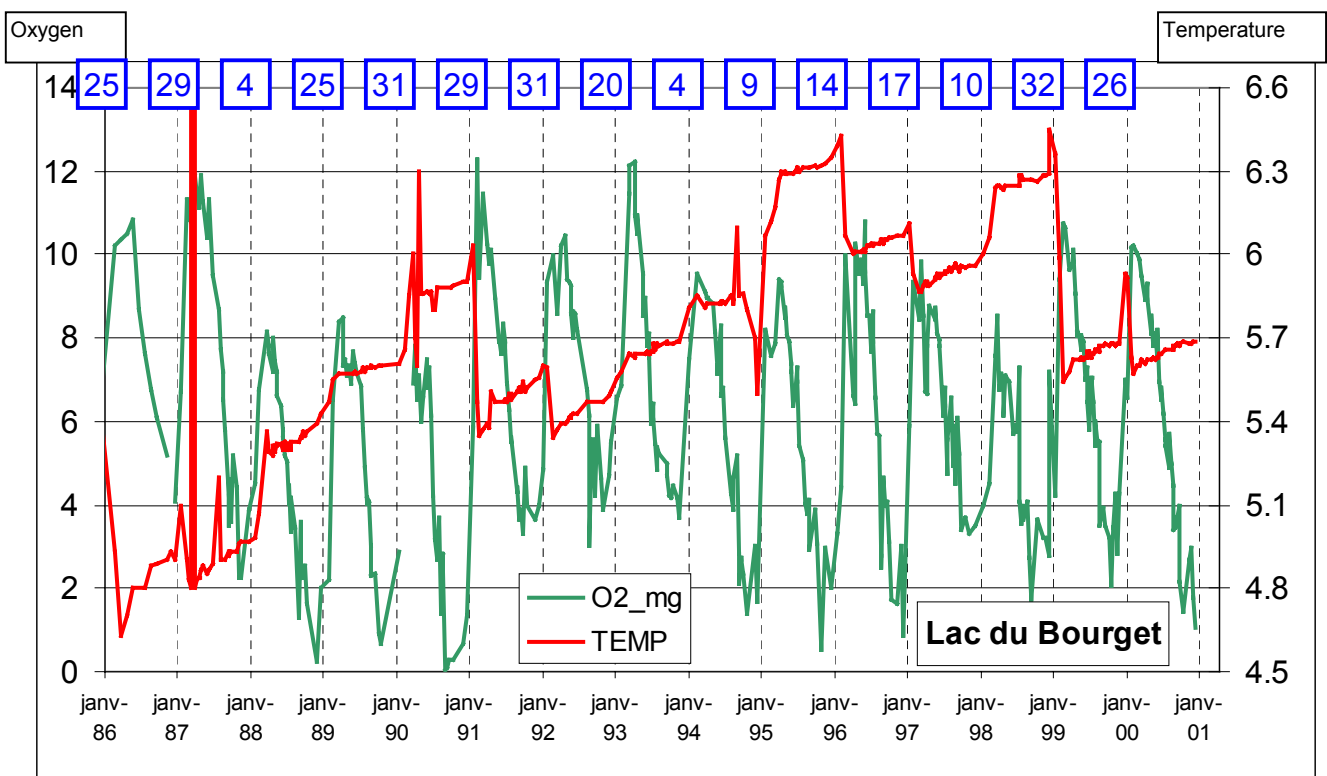


Figure 5.1 : Time series of the temperature and the oxygen in the deeper part of the Bourget Lake (-130.0m). The lake frost days per winter seasons (top diagram in blue)

The temperatures of the Bourget Lake behave generally in the same way as in Upper Lake Constance (E. Hollan & H. Baumert 2002)

³ Author of PART III: Claude Gilbaud

⁴ Lake frost day : Daily average air temperature below 0°C.

We observe a global increase of the temperature of the deep water during this period in the same order of magnitude than in Upper Lake Constance (see Figure 5.). In this two deeper lakes, in comparison with the Bourget Lake, the temperature is lower more than one degree.

During several winter the temperature of the deep water is falling down, generally when a number of lake frost days more than 30 days (1991, 1992, 1999 and 2001). In 1996 and 1997, the temperature is also decrease with a number of lake frost days about 15. These decrease are connected with the deep-water renewal due to winter convection.

The diagram (Figure 5.11) shows that the wintry oxygen maxima vary from year to year and are well below 10mg/l in certain winters. Therefore, we could interpret the situation that Bourget Lake shows an incomplete renewal in those years. On the other hand, the oxygen concentration during summer season is in the same order in the both lake (see Figure 5. 3).

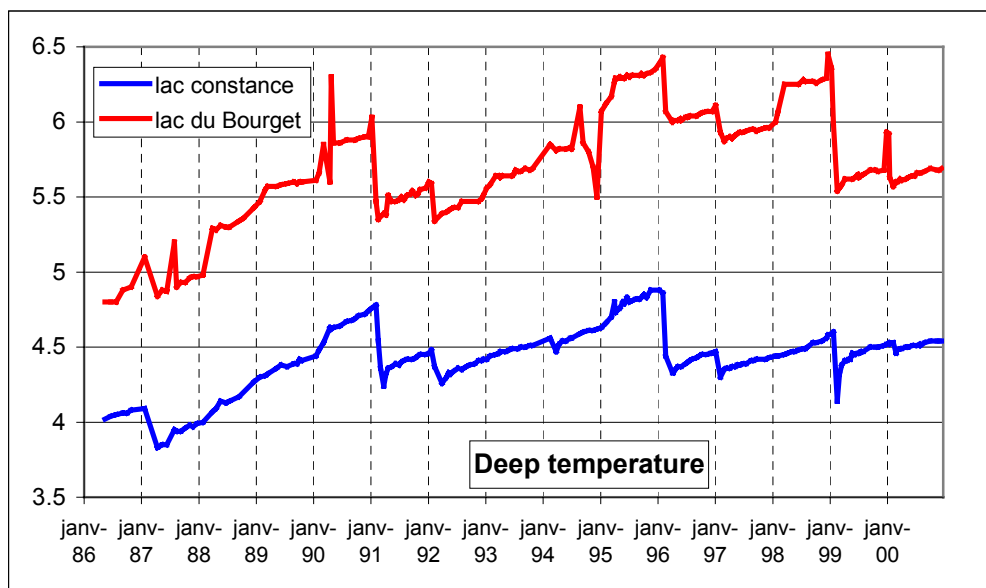


Figure 5.2: Comparison between the deep temperatures of Bourget Lake (red) and Lake Constance/Obersee (red).

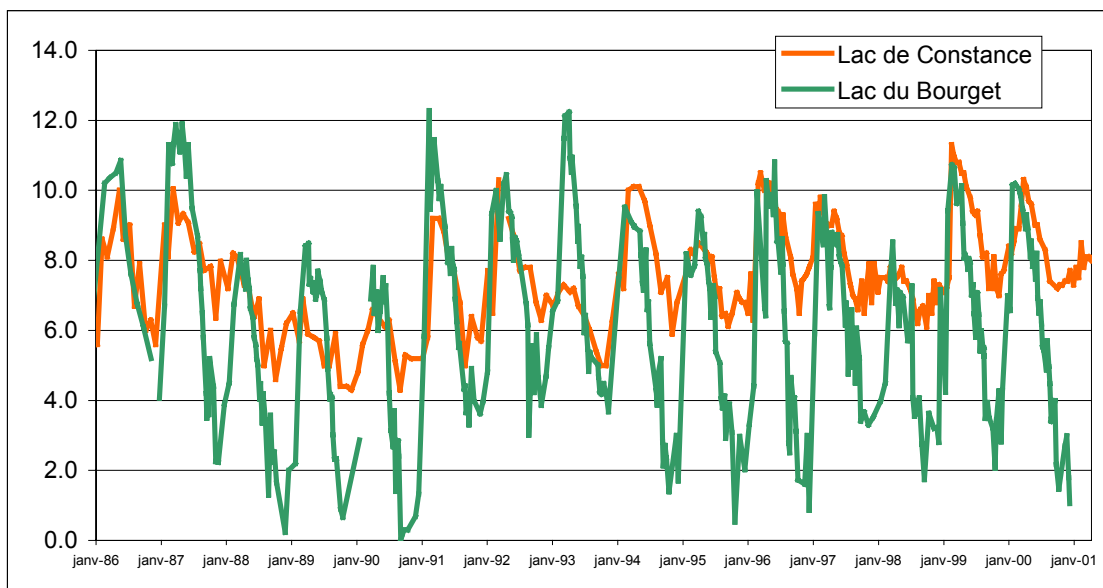


Figure 5.3 : Comparison between the deep oxygen contents in Bourget Lake (green) and Lake Constance/Obersee (orange).

5.2 BOURGET LAKE VERSUS UPPER LAKE CONSTANCE.

In the following table, we report the lake frost days per winter seasons for the both lakes.

	1986	1987	1988	1989	1990	1991	1992	1993	1994	1995	1996	1997	1998	1999	2000
Bourget Lake	25	29	4	25	31	29	31	20	4	9	14	17	10	32	26
Lake Constance	62	60	21	22	38	45	38	31	32	18	62	38	24	43	27

On the Figure 5.4, we have drawn the cross-correlation between the Bourget Lake and the Upper Lake Constance of the deeper lake temperature between 1986 and 2001. The black line is the linear regression (equation and regression coefficient are plotted on the figure).

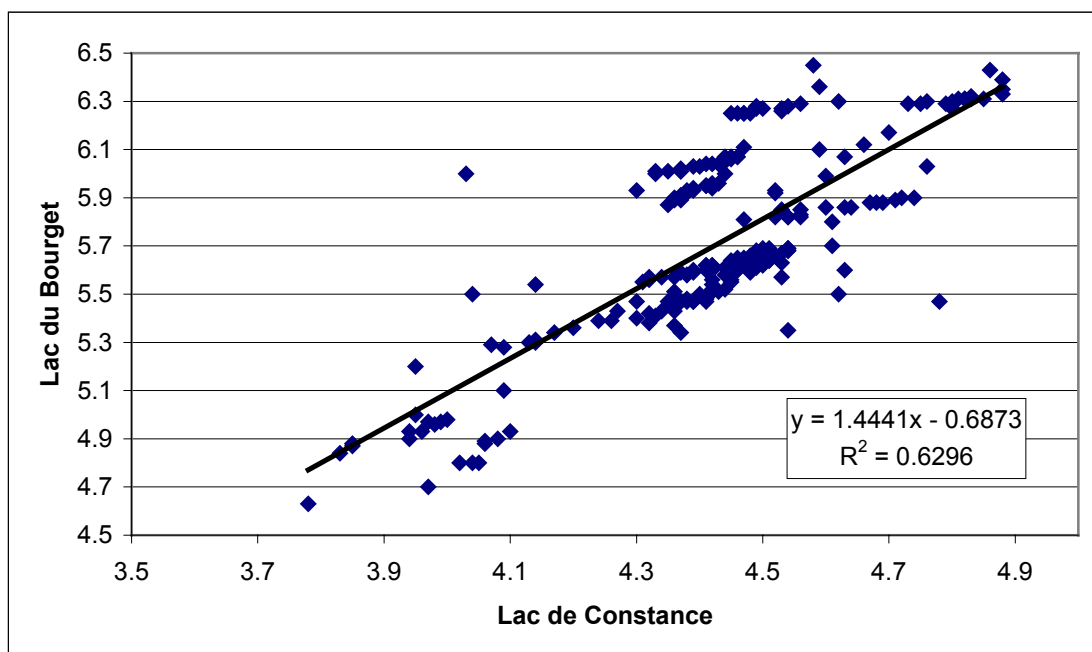


Figure 5.4 : Cross-correlation between the temperature of the Lac de Constance and the Bourget Lake (all data - Figure 5.).

On the Figure 5.5, we have drawn the deep lakes temperature, but the Bourget Lake temperature is shifted by -1.2°C . And then we redraw the cross-correlation between 1988 and 1995 on the Figure 5.6. Put share has few dots which are not on the line, the data are in a good correlation during this period.

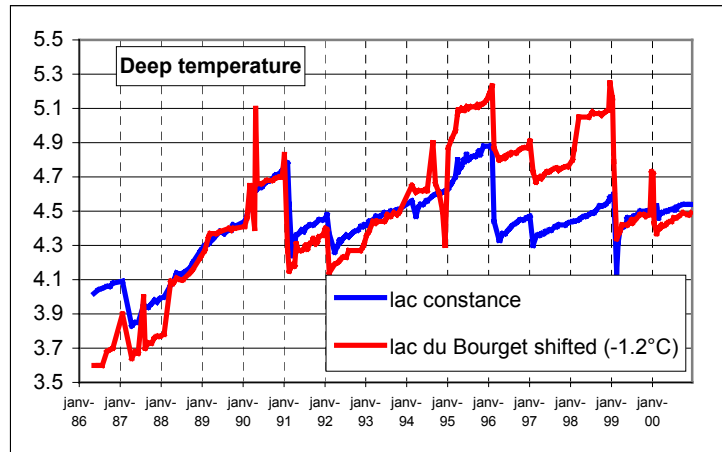


Figure 5.4 : Same as Figure 5., Bourget Lake temperature shifted by 1.2°C.

This tends to say, in regard to the deep-water temperature, that the two lakes are very similar respond to the climatic forcing between 1988 and 1995. The shift in the data (1.2°C) is constant during this period. But between 1996 and 1999, a new evolution, probably in the Bourget Lake, is observed, the shift is close to 1.6°C. Then after 1999, the evolution tends to come back to the first one.

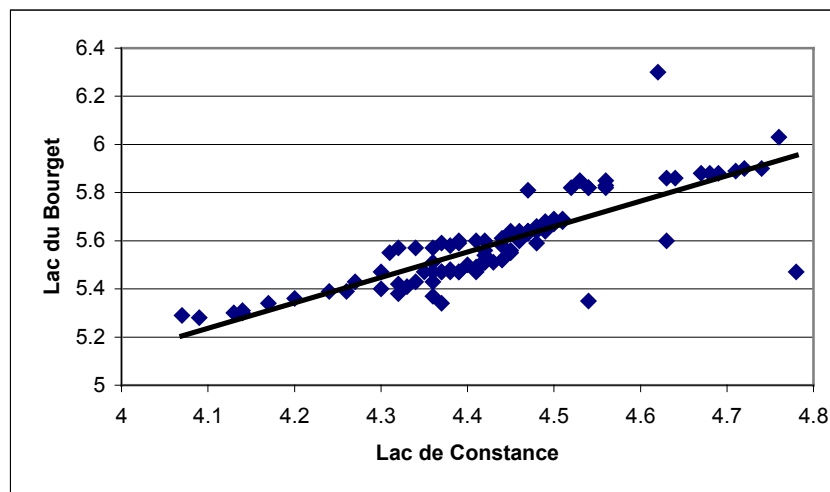


Figure 5.5 : Cross-correlation between the Celsius temperatures of Lake Constance and Bourget Lake for the period 03/1988-07/1994.

If we plot, in the same idea, the cross-correlation for the oxygen (Figure 5.5) between Bourget Lake and Upper Lake Constance for the period between 1986 and 2001, the pattern is completely different.

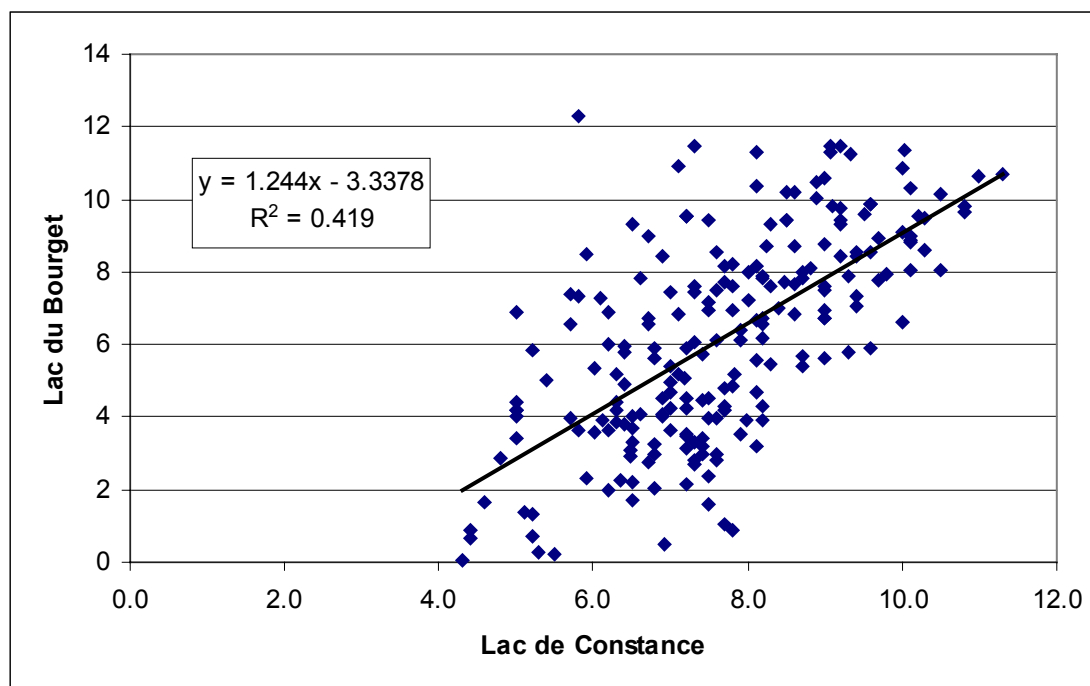


Figure 5.6 : Cross-correlation between the deep oxygen content of Lake Constance and Bourget Lake (all data -Figure 5. 33). Units on the x and y axis are mg l⁻¹

5.3 CONCLUSIONS

Regarding the latitude (Bourget Lake : 45°44' N – Lake Constance 47°39' N), the maximum depth (Bourget Lake : 145.0m – Upper Lake Constance : 252.0m) and the altitude (Bourget Lake : 231.0m – Upper Lake Constance : 395.0m) of the both lakes we expected very different behavior for the water deep temperature and oxygen concentration.

The temperatures, between 1986 and 2001, of the Bourget Lake behave generally in the same way as in Upper Lake Constance; the summer value of the oxygen concentration as well. The wintry oxygen is generally lower in the Bourget Lake than in the Lake Constance. The fluctuation of the oxygen concentration in the Bourget Lake (0.0 mg/l to 12.0 mg/l) is bigger than in the Lake Constance (4.0 mg/l to 10.0 mg/l), this is probably due to the lower depth of the Bourget Lake.

The temperature deep-water evolution of the Bourget Lake is a good indicator to the renewal of the lake deep-water. The oxygen concentration of the deep-water is adding information that the renewal is not complete each winter convective event (E. Hollan & H. Baumert; personal communication).

Regarding the deep-water temperature, the two lakes are very similar respond to the climatic forcing between 1988 and 1995.

6 PART IV: ECOLE POLYTECHNIQUE FEDERALE LAUSANNE

Stratification in Lake Geneva⁵

6.1 INTRODUCTION

Lake Geneva may be classified as a large deep lake. It is large because the Coriolis force is important in the force balance and it is deep because it does not destratify on a regular annual basis as will be shown below. It is about 70 km long and consists of two basins. The large and deep main basin (Grand Lac) is about 10 km wide and about 310 m deep in the central part. A narrower (Petit Lac; 4 km wide; 20 km long) and shallower (maximum depth 70 m) basin forms the western end. Details about the lake and its catchment area can be found in reports to D5 (WP30), D12 (WP14) and D2 (WP23).

Three aspects of hydrodynamics, i.e. the dynamical state, the physical mechanism and the energy level are very important elements in understanding problems of turbulent mixing and the formation of vertical thermal stratification. The result of the stratification is the formation of the seasonal thermocline. The force balance and the dynamics of the thermocline formation are presented in our report to WP9. Based in measurements carried out by our laboratory and data available from other sources, we will briefly present some features of all three aspects related to stratification in Lake Geneva. Key processes which may influence the thermal stratification of the lake have also been dealt with in detail in the reports to WP3, WP6, WP7, and WP8.

6.2 LAKE STRATIFICATION DYNAMICS

Lake Geneva is located in the central European climate belt which is characterised by strong seasonal changes in heat flux with hot summers and cold winters. Air temperature may be taken as a surrogate for heat flux. The seasonal variation of two-week mean air temperature at Pully (above Lausanne) over the last 15 years is shown in Figure 6-1: Two-week mean air temperature at Pully (above Lausanne; from CIPEL 2002). The range of air temperature change which is obvious from this figure will provide for a corresponding range in water temperature in the lake. In particular it should be noted that the air temperature falls below 4°C during wintertime. A seasonal variation in the water temperature and thus in the stratification in the lake can be expected.

⁵ Author of PART IV:
Dr. Ulrich Lemmin

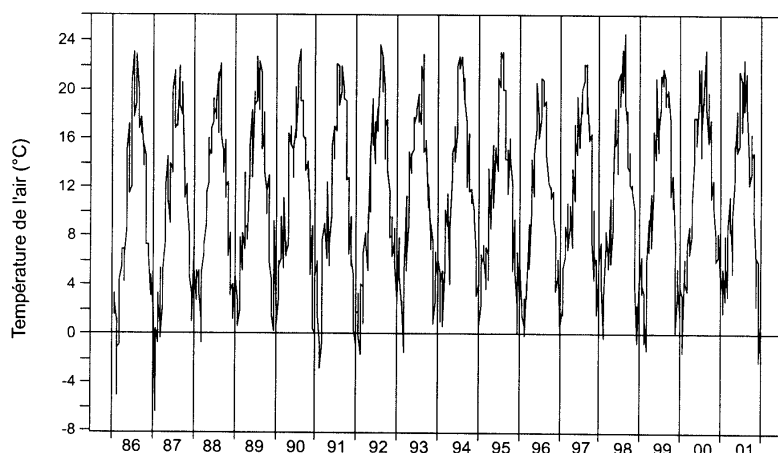


Figure 6-1: Two-week mean air temperature at Pully (above Lausanne; from CIPEL 2002)

In Figure 6-2 the heat content of the different layers of the water column in the centre of the Grand Lac basin has been plotted as function of time for several years. It can be seen that the seasonal variation of the air temperature is strongly reflected in the heat content of the upper 20m of the water column. In the two subsequent layers down to 80 m depth a regular seasonal pattern is still discernable. This regularity is lost for the remaining 200 m of the water column down to the bottom. A signal of strong winter cooling in early 1987 penetrates down to 130 m. Due to the high heat content of the upper 20 m layer, the total heat content of the lake shows a regular seasonal variation throughout the period of observation.

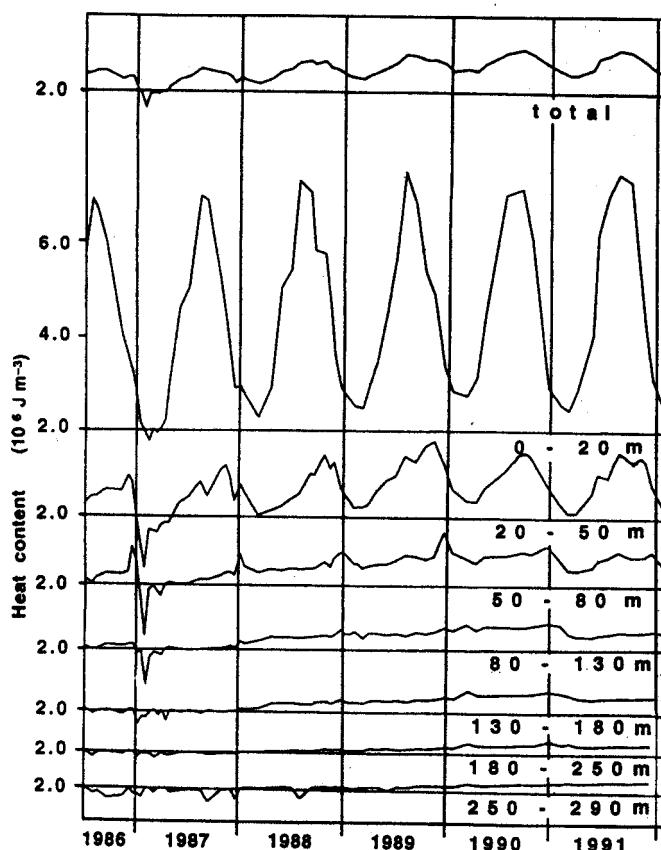


Figure 6-2: Heat content for different layers of the Grand Lac calculated from twice monthly temperature profiles taken in the center of the Grand Lac basin

From this analysis it is apparent that the seasonal stratification cycle of the lake is limited to the upper 100m of the water column. The heat content of all layers in Fig. 6-2 including the layers below 100m, continuously decreases for the whole period of observation used in this analysis. This means that the lake remained permanently stratified during this period. In order to investigate whether this is a significant feature of the stratification dynamics of Lake Geneva, the much longer time series of temperature data of the CIPEL was analysed. Mean values were calculated for each month separately.

The results are given in Figure 6-3 where selected isolines have been drawn to present the pattern. From this figure it is obvious that the Lake of Geneva does not destratify. The strong thermal stratification which is established during the summer months is limited to the upper 50 m of the water column. It is noted that throughout this summer stratification period a thermal gradient remains in this upper layer. Therefore, a well mixed epilimnion which is frequently invoked in lake stratification concepts does not develop in Lake Geneva. This indicates that wind forcing over this lake is not very strong. Below this layer isotherms may vertically shift by 50 m. However the overall stratification profile in this layer does change significantly.

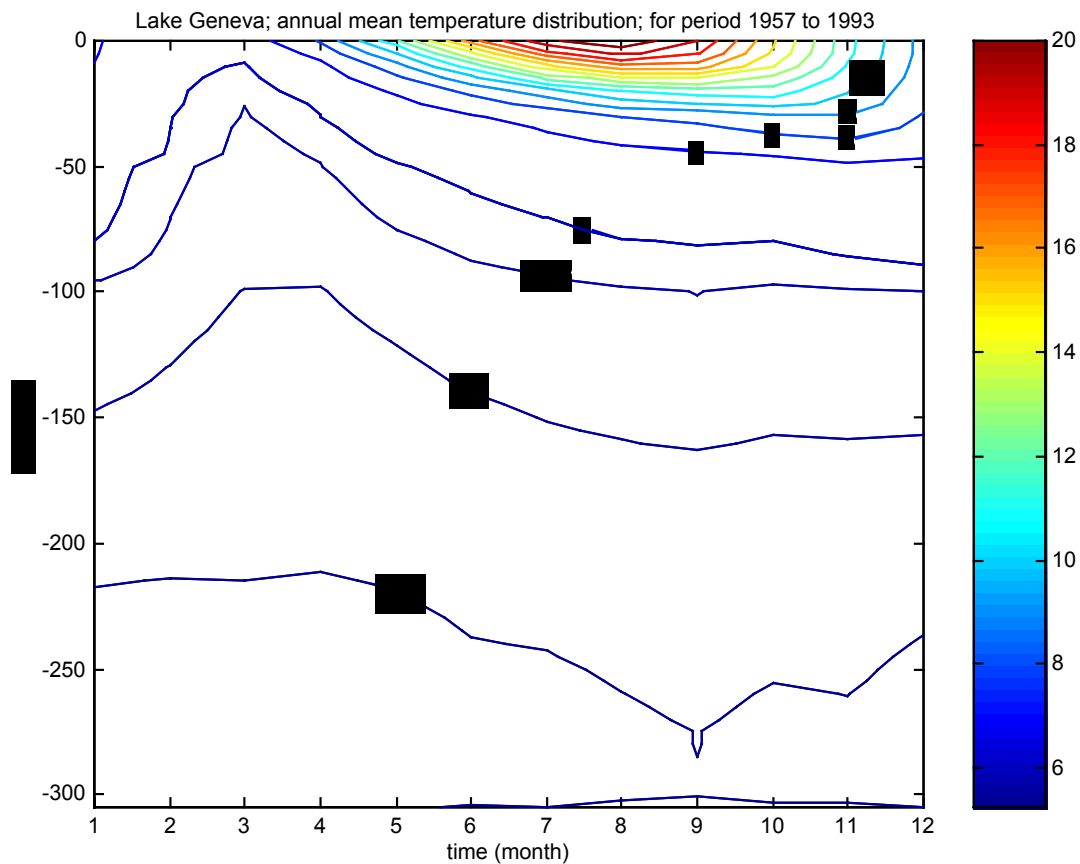


Figure 6-3: Mean monthly stratification calculated from monthly temperature profiles for the period 1957 -1993. The color bar on the right indicates the temperatures in °C. (data from CIPEL)

The weakest vertical gradient of less than 1°C is observed during the early months of the year. The water temperature which follows the air temperature pattern (Figure 6-3) will not reach the maximum density at 4°C even though the air temperature falls regularly below that value during wintertime (Figure 6-1). This indicates that for typical air temperatures in the Lake Geneva basin area, the heat loss from the lake to the atmosphere is not sufficient to provide for regular destratification. In this respect the generally low wind speeds mentioned above will also contribute to low heat exchange.

6.3 THERMOCLINE DEPTH

In order to establish the thermocline depth from this stratification pattern, the mean monthly Brunt-Vaisala frequency profile was calculated from the same data set. The Brunt-Vaisala frequency or buoyancy frequency N is defined as $N^2 = g \rho^{-1} (\partial\rho/\partial z)$. ρ is the water density which is a function of temperature and z is the vertical coordinate.

The pattern is plotted in Fig. 6-4 for the upper 35 m of the water column. The seasonal change in the Brunt-Vaisala frequency distribution reflects the changing mean stratification. Strongest stratification is found at the end of July. The regions of strongest vertical gradients for each month are marked by dots in the diagram. During the early season from March to May the location of the strongest gradients is found from the supplementary temperature profiles taken by the LRH because the resolution of the CIPEL data is not sufficient.

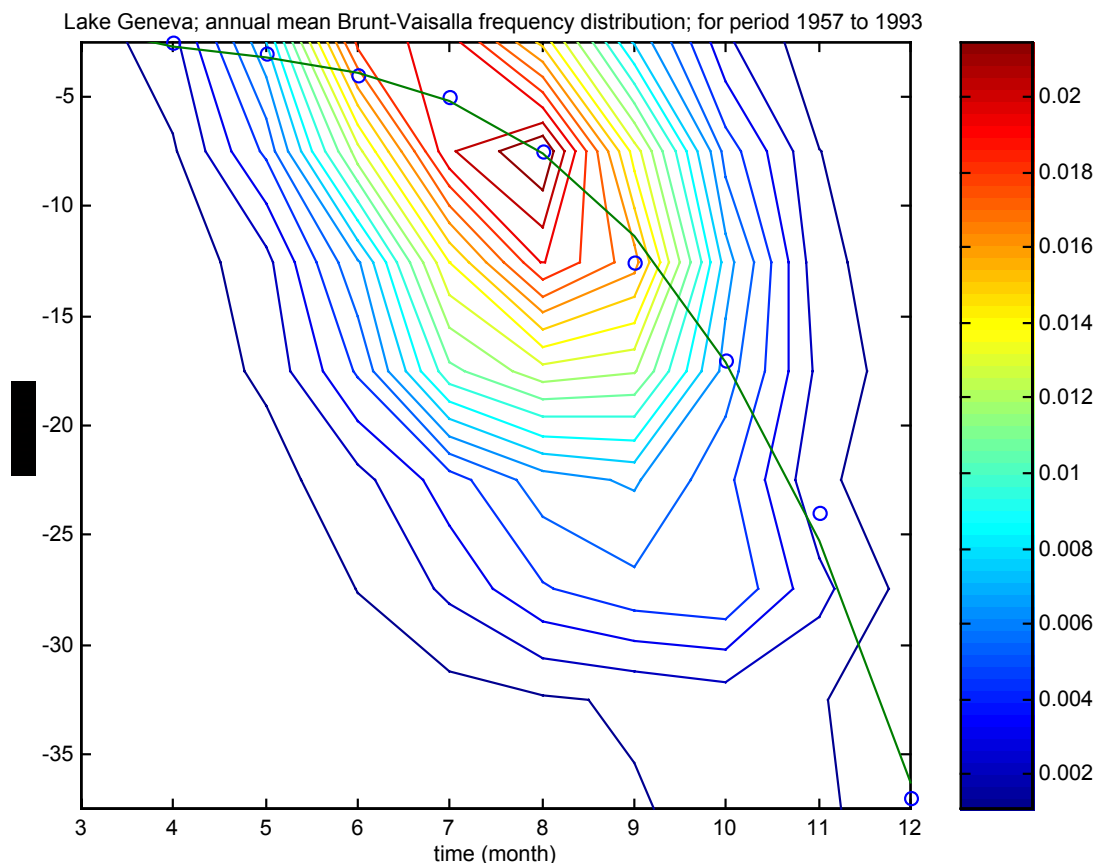


Figure 6-4: Mean Brunt Väisälä frequency distribution calculated from the mean temperature profiles given in Fig 3. Note the change in the depth scale. The color bar on the right indicates the Brunt- Vaisala frequency in cps

A curve has been fitted through these points to indicate the change in thermocline depth during the period of sufficiently strong stratification. The curve can be expressed as:

$$\text{Thermocline depth} = -0.0749 + 1.0504 \text{ month} - 5.4376 \text{ month}^2 + 7.0727 \text{ month}^3$$

This is an approximation for a longterm mean depth of the thermocline and may serve as a rough indication of the thermocline dynamics. This information may be of use in the managerial concept of the lake. The actual thermocline depth may however deviate

strongly from this mean depth as is detailed in our contribution to the WP 9 report. In that report it is also shown that within the lake basin at any given time, the thermocline depth may vary by a factor of two. While this is significant from the physical point of view it may not be very important for managerial questions which address longterm development.

6.4 MIXING DYNAMICS

Mixing dynamics is of great importance to the management of water quality because it affects water pollution prediction in relation to thermal stratification. In particular vertical mixing is an important aspect with respect to the exchange processes of heat and matter between the different vertical layers of the lake. It is controlled by atmospheric forcing at the water surface and the resultant advective and oscillatory motions in the water column. Generally speaking, the intensity of vertical mixing decreases with depth, making it difficult to measure and quantify the process in the great depths of those lakes where the surface area to depth ratio is small as it is for Lake Geneva (Zhang et al. 1994). On the other hand the concepts developed for the hypolimnion of shallow lakes may not be directly applicable to the deep layers of deep lakes. In addition the mixing created by density current exchange between near shore zone or lake branches and the main body may play an important role (see our report to WP6 and WP8).

Traditionally, mixing is expressed in terms of a turbulent mixing coefficient in analogy to the molecular diffusion coefficient. The turbulent coefficients are a measure of the intensity of the process and may subsequently be used in calculations related to water quality and heat transport. Mixing can be assessed either directly from microstructure measurements of the turbulence levels or indirectly by measuring temporal changes of the spatial gradients of some particular properties such as temperature. Correspondingly, mixing coefficients can be determined in two different ways. In the past, the indirect method (heat budget or flux gradient method) has frequently been applied to lakes. Mixing coefficients calculated by this method will be called effective mixing coefficients in this report. We have described the application of this method to Lake Geneva in our report to WP7. This method largely fails in the deep hypolimnion where spatial and temporal gradients become very small.

Thorpe (1987) first suggested that the mixing coefficient could be determined by treating individual vertical profiles of vertical resolution down to micro-scales. Mixing coefficients obtained by this method will be called active coefficients to distinguish them from the effective ones defined above. Micro-scale measurements in lakes have been carried out down to 50m depth (e.g. Imberger and Patterson 1990; Imberger and Ivey 1991) Based on this type of measurement it was revealed that turbulence can be characterised as active, decaying or fossil, as was already found in oceans. In the hypolimnion one finds few thin layers of active turbulence within the thicker layers of quiet waters. No micro-scale measurements from deep lakes appear to exist.

Vertical mixing is often complicated by density stratification, i.e. the existence of a thermocline with a strong gradient in lakes and reservoirs. This internal structure has a considerable influence on the flow field, turbulent mixing and dispersion. This stratification expresses a vertical force that may change the geometrical form of the eddies and restrict the vertical motion, and is traditionally quantified by the buoyancy frequency N .

The Thorpe displacement, d , is a measure for the vertical displacement of a small water volume caused by the turbulent motions before significant molecular diffusion has occurred (Thorpe, 1977 where also details of the calculation procedure can also be found). It can characterise the nature of the disturbance by identifying the level of origin of the unstable fluid and provide estimates of the potential energy involved in the mixing process. Turbulent mixing theories often depend on an assumption about the length scale of turbulent eddies. Thorpe (1977) proposed an objective method of estimating a length scale, the Thorpe scale L_T , associated with overturning events in a stratified fluid. The Thorpe scale is the rms Thorpe displacement averaged over a certain depth range Δz . It is proportional to the mean eddy size as long as the mean horizontal density gradient is much smaller than the vertical gradient (Dillon, 1982).

The turbulent cascade is often related to the structure of the turbulence. The cascade process only occurs in the volumes occupied by cascading eddies, i.e. turbulent energy only dissipates in turbulent volumes. In lakes, shear patterns may lead to regions of high dissipation surrounded by nearly irrotational fluid. This state of the fluid is termed internal intermittency. The inversion structures observed in vertical temperature profiles can be considered as indicators of this intermittency.

The analysis for Lake Geneva was carried out using profiles taken one or twice a month over several years at several stations (S1, S2, and S3) located on the central plateau of the Grand Lac basin of the lake. Following the results of the stratification dynamics (Figure 6-1), the lake was divided into an upper layer (above 80m depth) which is strongly affected by seasonal stratification and a lower layer for the remaining water column (Zhang and Lemmin). The results are summarised in Table 6-1.

Table 6.1: Thorpe scale, L_T , and inversion percentage, ζ , in different layers and different seasons (stations S1, S2 and S3, 1988-1993).

Layer	Season	L_T (m)	ζ (%)
Upper layer (above 80m)	Whole year	1.69	10.3
	Cooling season	3.41	18.7
	Heating season	0.59	4.9
Lower layer (below 80m)	Whole year	2.05	17.1
	Cooling season	2.36	19.4
	Heating season	1.83	15.5

Generally, the inversion structures (eddies) are larger during the cooling season than during the heating season for both layers. For the upper layer, however, the Thorpe scale during the cooling season is about seven times larger than the one during the heating season. Likewise, the inversion percentage shows a ratio of four between the

two seasons. For the lower layer the seasonal differences also exist but are much smaller. Thus, turbulent eddies may have nearly the same dynamical characteristics throughout total water column, whereas they show significant differences in the two layers during the heating season.

If the dissipation rate of kinetic energy does not change greatly, the Ozmidov scale, L_O , will be proportional to $N^{-2/3}$. Fig. 6-5 shows that the Thorpe scale in Lake Geneva can be approximated as a function of the buoyancy frequency and proportional to $N^{-2/3}$. The relationship $L_T \approx L_O$ suggested by Dillon (1982) is confirmed by our results over a wide range of buoyancy frequencies. Some scatter in the data is due to the instabilities in the profiles resulting from processes other than vertical turbulent overturns which at present cannot be eliminated from the analysis.

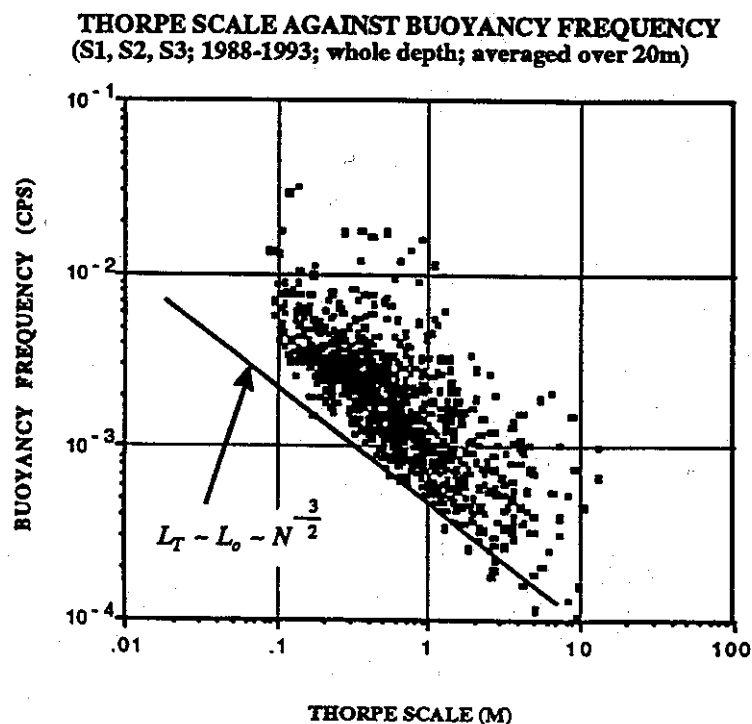


Figure 6-5: Thorpe scale as a function of buoyancy frequency

Consider an unstable range occupied by an inversion structure (or eddy) of size L_T . If the buoyancy frequency is N , the eddy mixing coefficient will be (Thorpe, 1987):

$$K_z(z) = 0.15 L_T^2(z) N(z)$$

As indicated above, it will be called active eddy (or mixing) coefficient. This equation will be used in the present calculation. In reality, the proportionality in this equation is a variable which may vary from 0.1 to 1000, and depends on the physical process energizing the turbulence (Ivey and Imberger, 1989). The eddy diffusion coefficient follows the following power law (Monin and Yaglom, 1975):

$$K = c l^{4/3}$$

where l is the length scale over which diffusion is measured. From the analysis of our data we obtained the following regression equations:

for the upper layer:
$$K_z = 2.88 L_T^{1.42}$$

for the lower layer:
$$K_z = 1.86 L_T^{1.44}$$

The value of constant c has been determined for individual layers and is found to be a function of depth (Fig. 6-6). This indicates that the mixing potential of an eddy of a given size decreases with depth. At 200 m depth it is reduced to about one half of its value at 40 m depth.

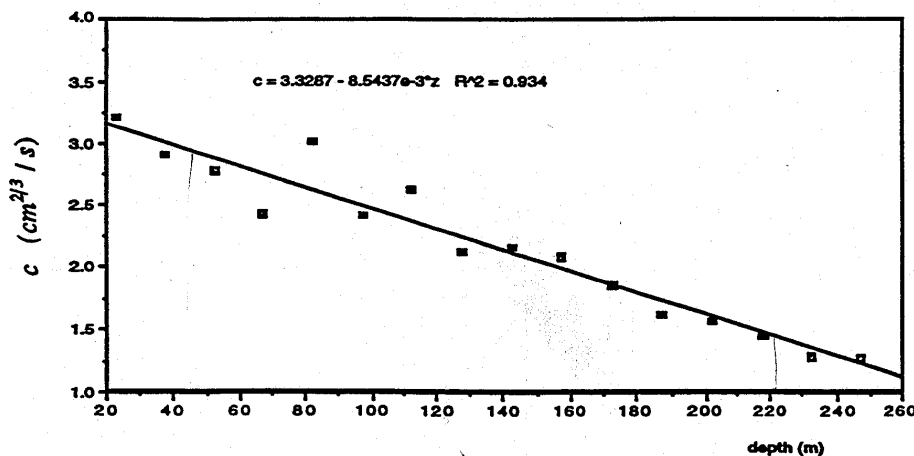


Figure 6-6: Constant c as function of depth (data from stations S1, S2 and S3; 1988-1993)

The Thorpe scale and the corresponding active eddy diffusion coefficient are then calculated for depth layers of 20 m thickness. The following regression equation is found from the analysis of all data:

$$K_z = 1.86 L_T^{1.34}$$

Note that the regression exponent is close to the 4/3 law given above. Results are shown in Fig. 6-7. It is evident that this law is valid for the mean condition of the active eddy coefficient for all profiles in the two layers and the whole year. The range of the validity from 0.1 m to almost 10m is much larger than the inertial subrange which the Kolmogorov theory indicates. A similar observation can be made for the range of applicability of the 4/3 law to horizontal eddy coefficients. We have investigated other data by Dillon (1982), Thorpe (1987), Gregg et al. (1994) and Wijesekera et al. (1993). Concerning the 4/3 law the results are in good agreement with the Lake Geneva data. However the constant is different.

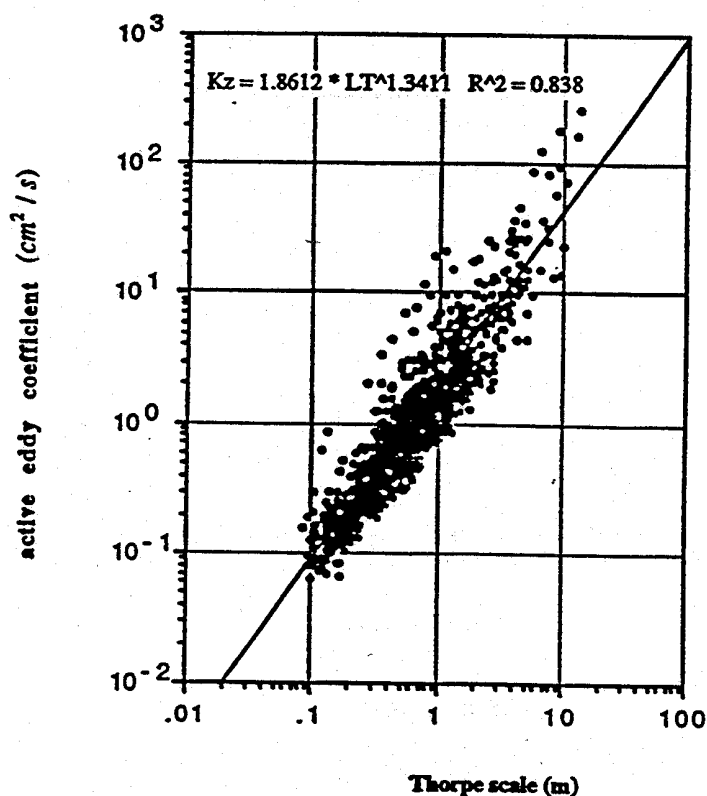


Figure 6-7: Active turbulent mixing coefficient as a function of the size of the inversion (Thorpe) scale. Data from stations S1, S2 and S3; 1988-1993; whole profile.

The active and the effective turbulent mixing coefficients have been compared for the heating season and the results are shown in Fig. 6-8. Physically, the effective mixing coefficient expresses the spatially and temporally averaged mixing whereas the active mixing coefficient characterises the potential energy or mixing ability stored in an instantaneous inversion structure (or overturning structure). Our results show that during the heating season the active coefficients are of the same order of magnitude as the effective ones obtained with the flux gradient method. In the simplest case, it can be assumed that the relationship between the two coefficients is determined by the inversion percentage for the range under consideration.

Since the vertical heat transport is dominated by the temperature gradient within the stratified range, an N dependence of the effective coefficient is empirically accepted only in the strongly stratified upper layer (above 80 m depth), but not valid in the weakly stratified or non-stratified lower layer. The active coefficient depends on N . Thus, it follows the same tendency as N over the whole profile. Furthermore, the active eddy coefficient shows an L dependence over the whole profile.

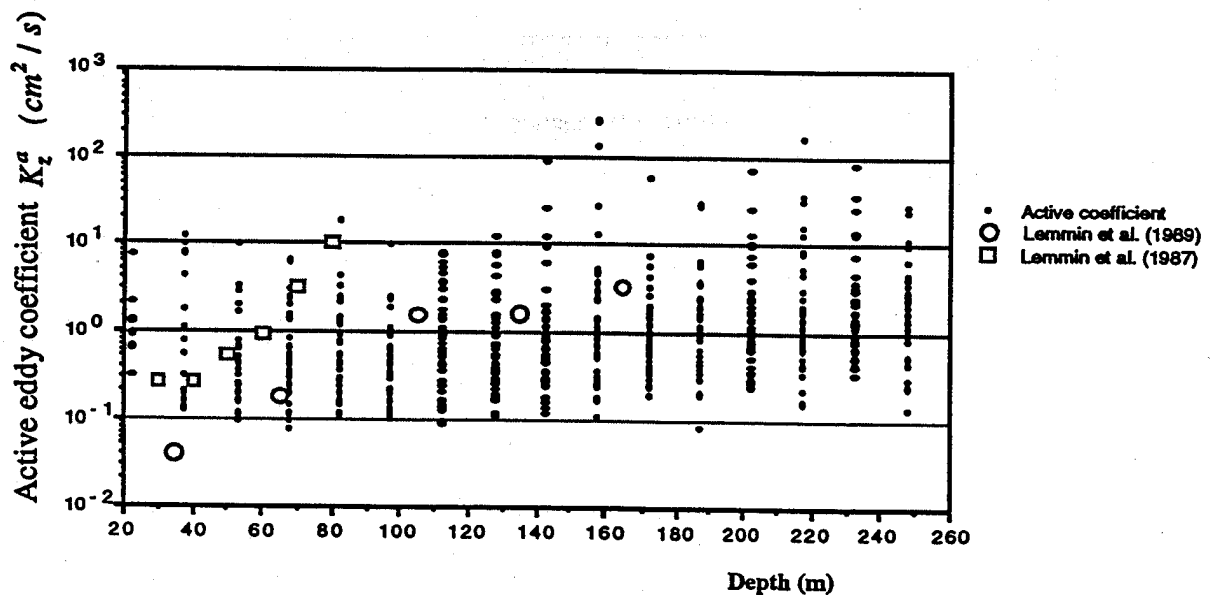


Figure 6-8: Active eddy coefficients as a function of depth compared with effective mixing coefficients obtained by the budget method (1987) and the flux gradient method (1989).

6.5 LONGTERM TRENDS

From the analysis of the water temperature timeseries in the center of the Grand Lac basin it had become obvious that the Lake of Geneva is characterised by a longterm mean stratification (Fig. 3). In order to investigate whether this mean state can be considered a steady state around which the actual annual stratification pattern oscillates, the longterm temperature patterns at selected depths were analyzed based on profiles measured at this station. These were presented in the most recent CIPEL report (CIPEL, 2002).

Annual mean temperatures for the period 1970 to 2001 at 5 m depth are shown in Fig. 6-9. The temperature data exhibit inter-annual fluctuations. The inter-annual fluctuations are not completely random but instead are dominated by a cyclic pattern with a repeatability of four to seven years. The mean amplitude of this cyclic pattern is slightly larger than 1°C. The cyclic pattern can be related to the variation in heat flux seen in the air temperature pattern in Fig. 6-1. From Fig. 6-1 the most obvious inter annual differences in heat flux appear during low temperature periods in winter. A longterm trend line with a slope of about 1°C/30 years has been drawn through this temperature pattern. No detailed analysis has been carried out yet. However, the air temperature timeseries in Fig. 6-9 indicate a slight trend in the low winter temperatures during the last few years. Thus, a longterm trend is superimposed on the cyclic variation. Since these results are based on annual mean temperatures, the trend as well as the cyclic pattern can be considered as significant.

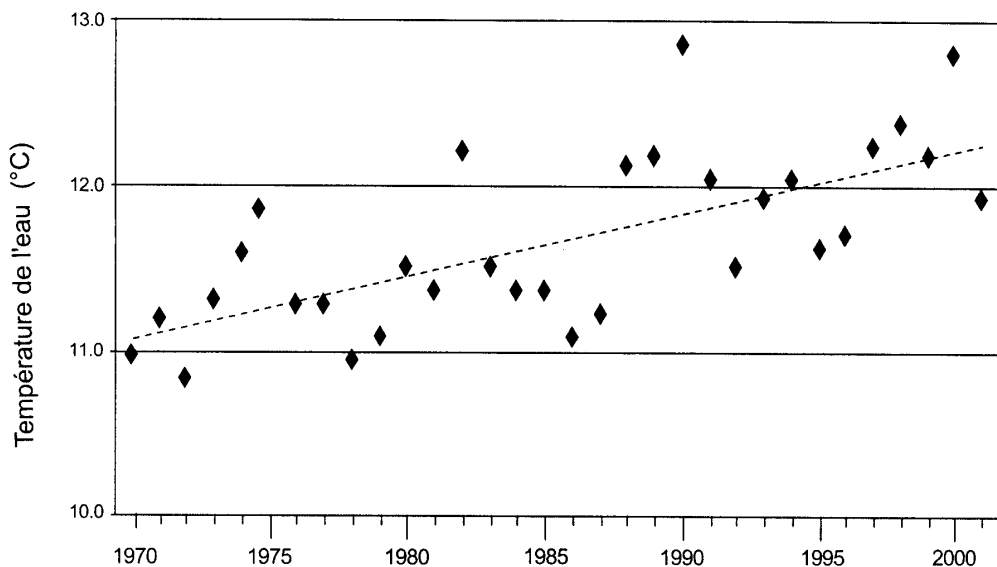


Figure 6-9: Trend of annual mean water temperature in 5 m depth based on monthly temperature profiles taken in the center of the Grand Lac basin of the Lake of Geneva (from CIPEL, 2002).

The annual mean temperature data in the deepwater layers has been presented in Fig. 6-10. A cyclic pattern similar to that seen at the 5 m depth is also found at greater depth. However, the four to seven year cycle only penetrates down to 100m and at that depth it has a smaller amplitude than at the 5 m depth. This corresponds to the observation above that the annual variability is limited to the upper 100 m thick layer. Peak values at the 5m depth occur often (but not always) a year ahead of those seen at 100 m depth. In the deeper layers the variability is strongly marked by the years of significant cooling (1965, 1971 and 1987) which can be related to winters with lower than average mean temperature. However, it should be noted that there is an important difference in the gradient structure in the years ahead of the minimum.

The trend line shown at the 5 m depth (Fig. 6-9) has been redrawn by eye in Fig. 6-10. A statistical analysis will be needed to determine the correct slope of this line. However, it appears that the correct slope will not be very different from the one drawn here. One can therefore assume that the whole lake has been following a warming which is close to this trend. For the deepwater layers below 100 m depth, this tendency is quite obvious for the last fifteen years (1987 to 2002). The mean gradient is very similar at all three depths which are shown in Fig. 6-10. However, this gradient is higher than one would find at the 5 m depth. Thus, the deepwater layers respond different from the upper layers to the present climate pattern. It can also be observed in Fig. 6-10 that during the whole period, even during winters with strong cooling, the layer below 100m depth remains stratified in the annual mean. This confirms that the longterm mean pattern shown in Fig. 6-3 is also valid on an annual basis.

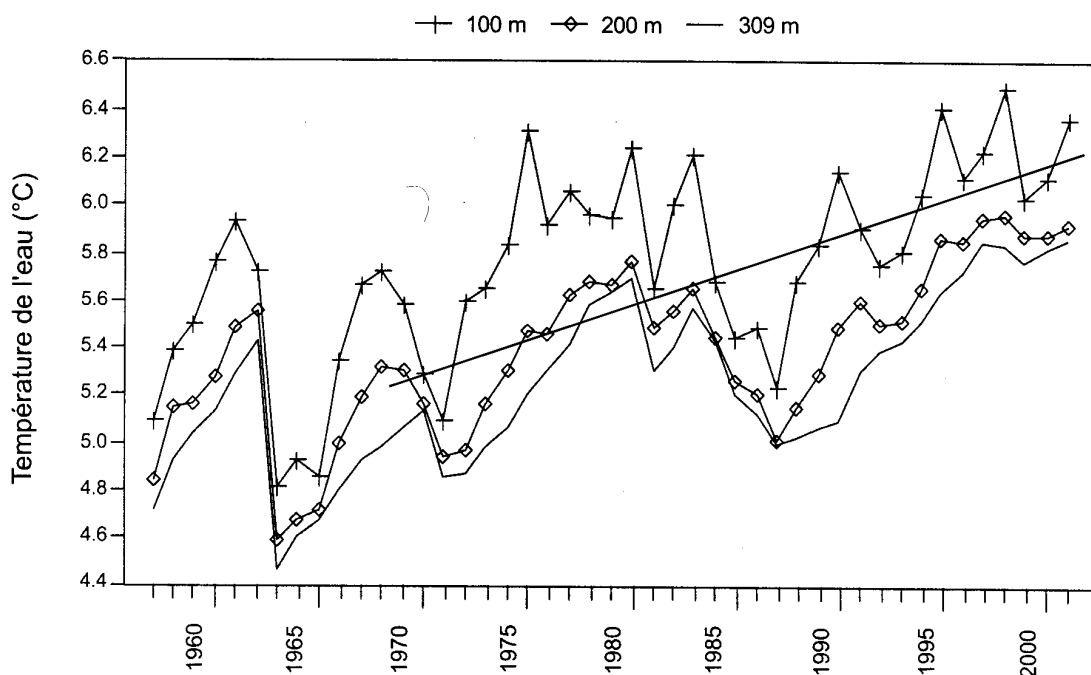


Figure 6-10: Annual mean temperature at the center of the Grand Lac basin for different depths (modified from CIPEL 2002).

6.6 CONCLUSIONS

Temperature profile data collected in the central part of the Grand Lac basin of the Lake of Geneva have been used for an analysis of some aspects related to stratification dynamics. It has been shown that in the longterm mean the Lake of Geneva remains permanently stratified. It is found that this is not a steady state situation. Interannual variations occur which, however, are not completely random. Instead, multiannual cyclic variations which can be related to the variation in atmospheric heat flux are found. Superimposed on this cyclic pattern is a longterm trend of warming. While this is seen in the whole water column, the gradient in the upper layer is different from that in the lower layer.

The effect of this stratification dynamics is that oxygen renewal to saturation level in the deep layers of Lake Geneva occurs only sporadically during 'exceptionally' cold winters. Since these winters occur only at long time intervals, oxygen concentration falls rapidly to low levels due to oxygen demand from the sediments and remains there. However, a certain renewal occurs every year even though the lake remained stratified during the cooling season. This indicates that processes other than vertical mixing contribute to deepwater renewal. We have discussed river plumes and lateral convective cooling as possible contributors in the reports to WP6 and WP8.

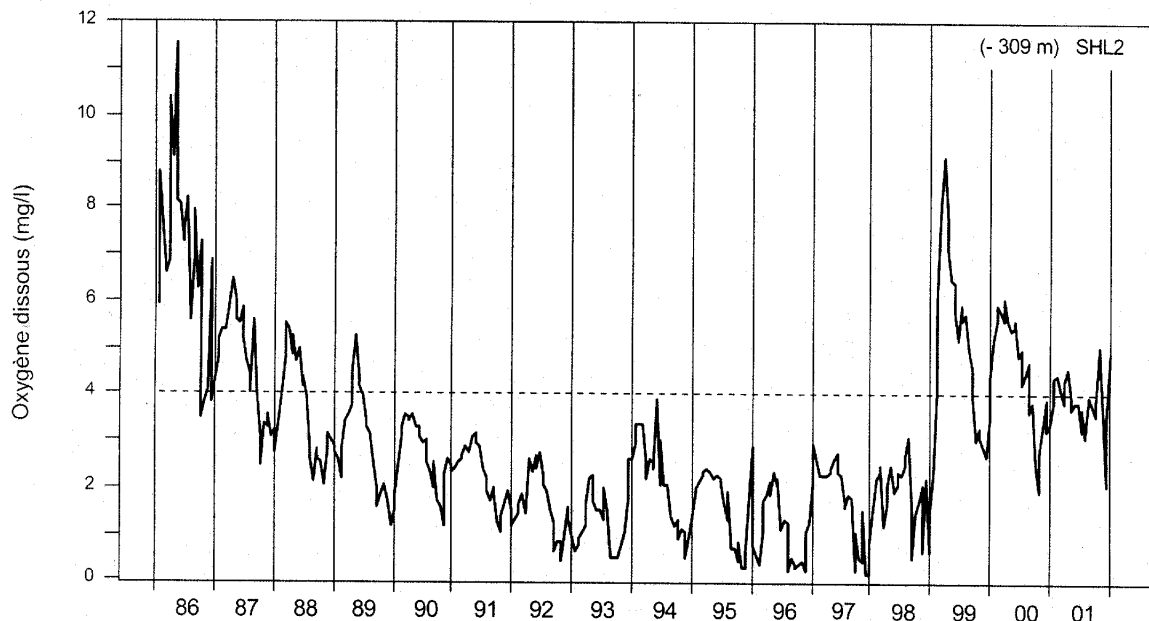


Figure 6-11: Oxygen concentration near the bottom of the Grand Lac basin of the Lake of Geneva (from CIPEL, 2002)

The longterm trend towards warming may have an opposite effect on the stratification dynamics. As was seen in Fig. 6-3, the temperatures below 100 m change very little throughout the year. Due to the longterm warming trend they are now approaching 6°C. On the other hand, we know from our measurements that under the present climate pattern, temperatures in the upper part of the water column may decrease to about 6°C during the later part of the winter. Due to this pattern, the probability of destratification will rise in the near future as long as the present rate of atmospheric warming will not change. This has been discussed in Lemmin (1998).

The dynamics of seasonal stratification are strongly controlled by the state of turbulence in the water column. We have shown that much can be learned about turbulence in Lake Geneva from the fine-scale CTD profiles which we have taken. Individual profiles provide sufficient information to characterise the state of turbulence and the potential of mixing. We have shown that if temperature inversions smaller than those which can be resolved with our instrument are neglected, about 15% of the water column is unstable and contributes to mixing at any given time. The inversion percentage is slightly higher during the cooling season than during the heating season.

For the stratified period, the active dissipation rate has a decreasing tendency with depth in the upper layer. For the weakly or non-stratified lower layer, the difference between the active and the average dissipation is quite small due to the large inversion percentage. The production of turbulent energy will be nearly constant in this layer because the rate of change of the available potential energy for mixing and the dissipation rate do not vary greatly with depth.

The mixing mechanisms in the strongly stratified upper layer and the weakly stratified lower layer are physically different. Within the stratified range, the vertical heat transport, coupled with atmospheric forcing at the water surface, is controlled by the density gradient. Thus, N-dependence of K_z is always verified by the heat budget method. For the weakly or non-stratified layer the mixing is not directly related to N. Instead, it is controlled by the size of the eddies and the mixing coefficient can be expressed by an L-dependence. We have shown that active mixing coefficient of an eddy of a certain size diminishes linearly with depth. This means that the mixing potential stored by a given eddy decreases with depth. Our measurements have verified existing turbulence observations. However, it has to be realised that for certain parameters, scatter may exist. This indicates that unstable inversions in the water column are not only produced by turbulent eddies. Other processes may be involved. Further studies will be needed to investigate these processes and quantify their importance in the determination of the stratification dynamics.

7 PART V: HYDROMOD SCIENTIFIC CONSULTING

On a new theory of stratified shear turbulence in lakes⁶

7.1 OVERVIEW

Based on detailed inspections of laboratory experiments carried out by *Dickey & Mellor* (1980) and by the group of *Van Atta* at the University of California at San Diego (*Rohr et al.* 1988, 1989; *Itsweire et al.* 1985) we analysed, rationalized and unified the existing turbulence models of the *Mellor-Yamada* and the *k-ε* class for the special but relatively simple setting of homogeneously stratified shear layers. For the simplified but realistic case of homogeneous shear layers we derived a "canonical" form which unites both classes. In canonical presentation those classes differ only in the choice of the model parameters (*Baumert & Peters* 2000). We found that - in their standard form which is widely used in geosciences - both classes do not correspond to the a.m. laboratory experiments. Further we found that (i) a certain choice of parameters leads to an agreement with the laboratory data within the limits of turbulence measurement the errors and (ii) there remains a contradiction in the turbulent kinetic energy balance (the steady-state Richardson number is not smaller than $\frac{1}{4}$) which can only be resolved by assuming that turbulence generates another energy form which does not contribute to mixing. Possible candidates are (a) the vortical mode and (b) internal waves generated by shear-driven turbulence. We concluded that (b) is the actual mechanism and included a corresponding term in the balance equation of turbulent kinetic energy. This solved all problems.

We continued our analysis by a study of boundary layers and concentrated our efforts on field observations by *Businger et al.* (1971), *Anis & Moum* (1995), *Drennan et al.* (1996) and *Terray et al.* (1996). We found that for a proper description of spatially inhomogeneous conditions the use of the *k-Ω* system of primary variables (for two-equation turbulence models) is better suited than the *k-ε* or other similar systems. For the *k-Ω* system we found that the von-Karman constant may be derived analytically as $(2\pi)^{1/2}$ and the Monin-Obukhov similarity function as $\Psi = 1 + 4\zeta$, where $\zeta = z/L_{MO}$ is the normalized distance to the boundary and L_{MO} the Monin-Obukhov length scale. The above Monin-Obukhov scaling could be derived as a solution for any system of primary variables if one restricts its validity to asymptotical distances from the boundary, i.e. to $z \gg L_{MO}$. The data show that the above scaling seemingly holds everywhere including regions very close to the boundary. We concluded that phenomenon can only be explained within the *k-Ω* system of primary variables if the action of the internal waves generated (besides turbulence) by the shear is taken into account, namely if the internal-wave drag is considered in the momentum balance and in the enstrophy balance.

⁶ Author of PART V:
Dr. *Helmut Baumert*

Due to the limited space in this report we have to refer to ANNEX A where the contribution of HYDROMOD is outlined and explained in greater detail.

We mention that our work on the physics of turbulence profited heavily from a parallel cooperation with Prof. H. Peters from RSMAS at U. Miami, Florida, within the framework of the EC CARTUM project, and from the exchange of experiences and views with Prof. E. D'Asaro/U. Washington and Prof. Mellor/U. Princeton.

7.2 SELECTED RESULTS

For homogeneously stratified shear layers our canonical two-equation turbulence model is described by the following relations:

$$\frac{dK_t}{dt} = P - B - W - \varepsilon, \quad (1)$$

$$\frac{d\varepsilon}{dt} = \left(\frac{3}{2} P - B - W - 2 \cdot \varepsilon \right) \varepsilon / K_t. \quad (2)$$

Here K_t is the turbulent kinetic energy, $P = -\langle \mathbf{u}' \cdot \mathbf{w}' \rangle \cdot \mathbf{S} = \nu_t \cdot \mathbf{S}^2$ and ε are its production and dissipation rates, respectively, S is the current shear, $\nu_t = c_\mu \cdot K_t^2 / \varepsilon$ is eddy viscosity. $B = g \langle w' \cdot \rho' \rangle / \rho_0 = \mu_t \cdot N^2$ is the potential energy flux of turbulence and W describes the generation of a certain 'non-mixing' form of energy. We assume that this form is the energy of in-coherent internal wave motions as early observed in experiments by *Townsend* (1965), *Wu* (1969), *Schooley and Hughes* (1972), *Woods and Wiley* (1972), see also *Barenblatt* (1978), *Barenblatt and Monin* (1979). Here μ_t is the eddy diffusivity related to the eddy viscosity by the turbulent Prandtl number σ as follows: $\mu_t = \nu_t / \sigma$.

In our new theory the notion *Collapse of turbulence* plays a key role. Based on analogy considerations with periodically forced oscillators under friction we postulate that turbulence collapses into internal waves if the characteristic time scale, τ , of the energy-containing turbulent eddies reaches half of the period of (potential) internal waves:

$$K_t \cdot N = \pi \cdot \varepsilon \quad \text{or} \quad \tau = K_t / \varepsilon = \pi / N$$

where N is the Brunt-Väisälä frequency and τ_c is the *collapse time scale*. In this sense the above relations (1) and (2) hold only as long as $\tau < \tau_c$. After the onset of the collapse at $\tau = \tau_c$ we assume that the dissipation rate decreases with an e-folding time of τ_c . This leads to the following modification of (2) for the time after the onset of the collapse (the TKE balance remains unchanged):

$$\frac{d\varepsilon}{dt} = \left(\frac{3}{2} P - B - W - 2 \cdot \varepsilon \right) / \tau_c. \quad (3)$$

Figures 6.4 and 6.5 exhibit a comparison with the famous experiment by *Dickey and Mellor* (1980) and some details of the collapse process as described by the above theory. In the simulations we assumed that the turbulence in this experiment is generated at $t = 0$ as a kind of white-noise process without correlation, in the absence of shear, so that $B = 0$ and $W = 0$.

Many laboratory experiments on stratified shear turbulence are carried out under conditions of exponential evolution (see *Rohr et al.* 1989) which we called structural equilibrium of turbulence (*Baumert and Peters* 2000). Mathematically it is characterised by $d\tau/dt = 0$. This condition is satisfied asymptotically in stratified shear layers when shear and stratification are held constant. Under those conditions the above theory reduces to the following simple relations:

$$\tau = \tau_\infty = \pi \cdot \sqrt{2} / S \quad (4)$$

$$(\tau/\tau_c)^2 = 2 \cdot R_g \quad (5)$$

$$L_{Th}/L_O = c \cdot 2^{3/4} \cdot R_g^{3/4} \quad (6)$$

$$v_t = 2 \cdot \varepsilon / S^2 \quad (7)$$

$$F_t = \sqrt{\frac{\pi}{2}} c^{-2} / R_g \quad (8)$$

where $\sigma = \sigma_0 / (1 - 2 \cdot R_g)$ and $c_\mu = \pi^{-2} \approx 0.101$. Here L_{Th} is the Thorpe scale, L_O the Ozmidov scale, R_g the gradient Richardson number and $\sigma_0 = 1/2$. Obviously, for $R_g \geq R_g^c = 1/2$ structural-equilibrium turbulence may not exist because of the collapse into internal waves. In terms of the turbulent Froude number the limitation $R_g < 1/2$ corresponds to the bound $F_t > \sqrt{\pi}/c$. The parameter c is here a quantity which relates the generic length scale L ,

$$L = c_\mu \cdot K_t^{3/4} / \varepsilon, \quad (9)$$

of the present theory to a specific measurement (or estimation) procedure for the turbulent master length scale which has been invented and described by *Thorpe* (1977). Therefore this parameter c is part of the measurement relations rather than being a generic part of the present theory. Figure 7-1 shows a comparison of relation (6) with observations from various sources (for the data and their origin see *Rohr et al.* 1989, *Schumann and Gerz* 1995 and *Baumert and Peters* 2000).

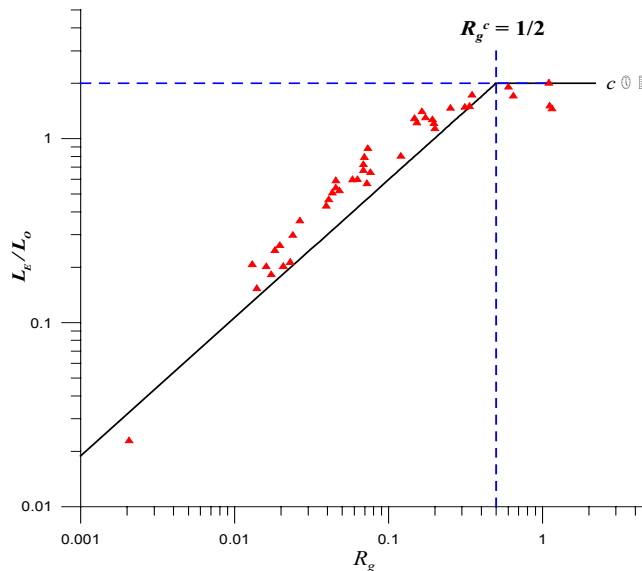


Figure 7-1: The ratio of the Ellison to the Ozmidov scale versus the gradient Richardson number in structural equilibrium.

Figure 7-2 shows a comparison of the flux Richardson number,

$$R_f = \frac{B'}{P} = \frac{\frac{g}{\rho_0} \langle w' \cdot \rho' \rangle}{\langle u' \cdot w' \rangle \cdot S} = \frac{c_{\mu'} \cdot N^2}{c_{\mu} \cdot S^2} = \frac{R_g}{\sigma}, \quad (10)$$

with observations, where we made use of relation (8).

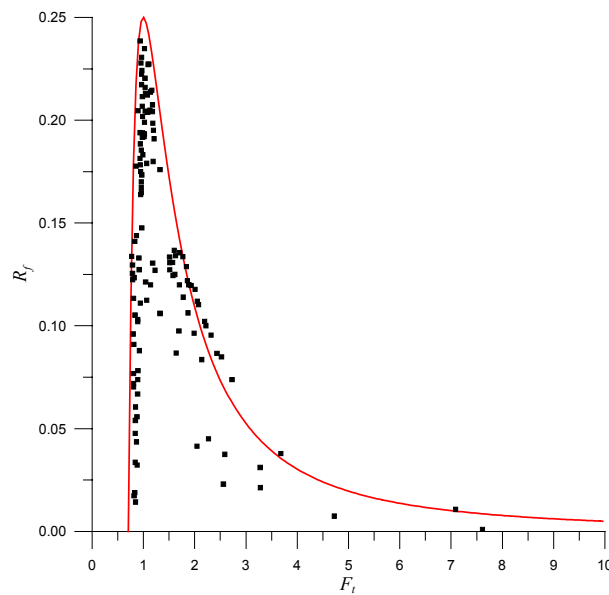


Figure 7-2: The flux Richardson number R_f as a function of the turbulent Froude number F_t . Symbols: observations reported by Ivey (1975, see also Imberger 1985); Full red line: present theory.

Figure 7-3 shows the behaviour of the functions B' and B which are mathematically given as

$$B = (1 - \varphi) \cdot \mu_t(0) \cdot N^2 \quad (11)$$

$$W = \varphi \cdot \mu_t(0) \cdot N^2 \quad (12)$$

such that $B + W = \mu_t(0) \cdot N^2$ where $\mu_t(0) = \nu_t / \sigma_0$ is the eddy diffusivity for neutral stratification. Figure 6.3 shows how the total flux is linearly splitted here into a mixing part, B , and a non-mixing part, W . Here $\varphi = (\tau / \tau_c)^2$.

In the case of full stationarity of turbulence (full equilibrium, $dK_t/dt = d\varepsilon/dt = 0$, Baumert and Peters 2000) the complete model for homogeneous shear layers exhibits the following properties,

$$R_g^s = R_f^s = \frac{1}{4}, \quad \sigma_s = 1, \quad (13)$$

in good agreement with common physical experience. We notice that all other current two-equation turbulence models like the $k-\epsilon$ model in its standard form and in the form discussed by *Burchard and Baumert* 1995 and also the Mellor-Yamada model in all its versions either contradict the properties (13) or exhibit major deviations from the observational data given in Figures 7-1, 7-2 and 7-4.

For details of the model discussed above we refer to ANNEX A to this report. For applications of the new closure (long-term climatological simulations of Loch Lomond in Scotland and Lake Constance in Germany) we refer to the Final Report to EUROLAKES WorkPackage 22 which is presented as EUROLAKES Deliverable D20.

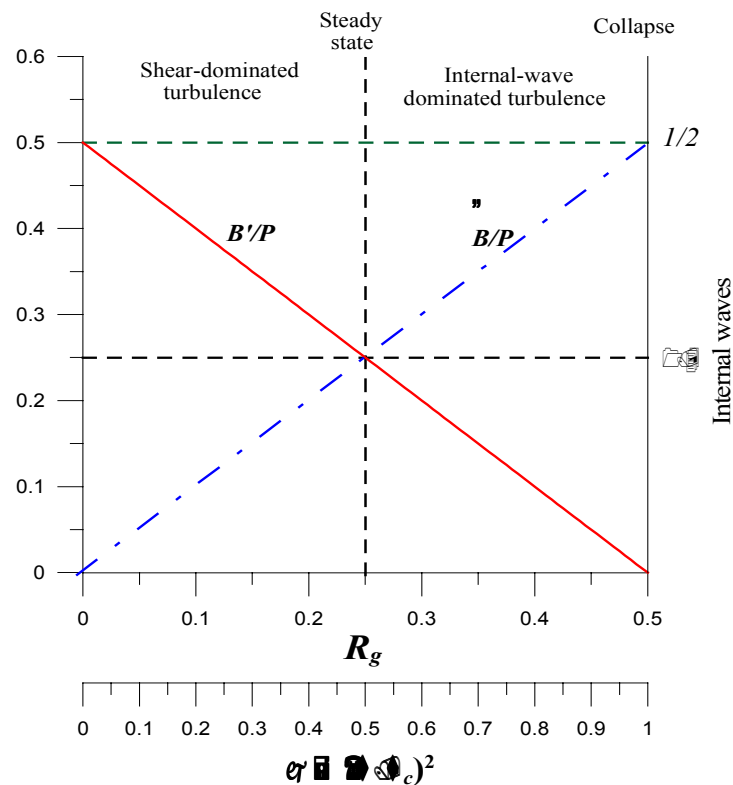


Figure 7-3: Splitting of the buoyancy flux into a turbulent (and mixing)

part B' (in our text notation: B) and a non-turbulent (non-mixing) part \tilde{B} (in our text notation: W).

The relation $\varphi = (\tau / \tau_c)^2 = 2R_g$ holds for structural equilibrium ($d\tau/dt = 0$).

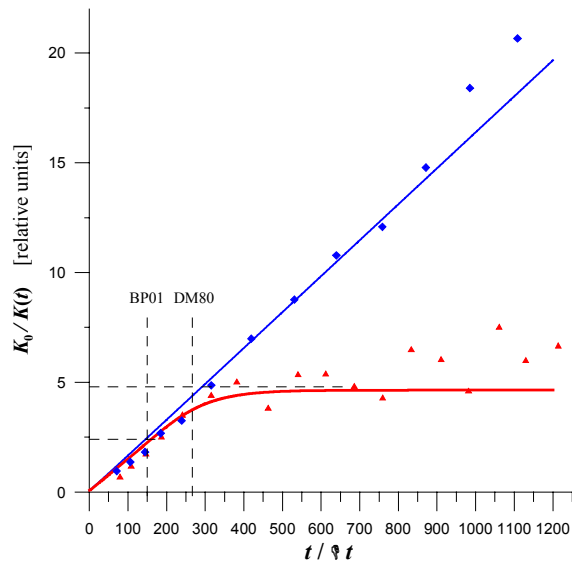


Figure 7-4: The collapse of turbulence in a stratified fluid.
Symbols: Observations by *Dickey and Mellor (1980)*; **full lines:** present theory. **Blue:** neutral stratification; **red:** stable.

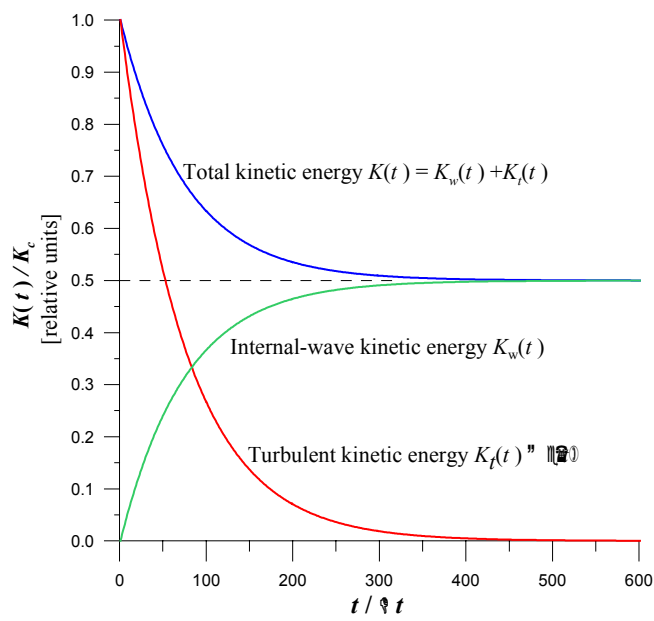


Figure 7-5: Details of collapsing turbulence after onset at $t = 0$.

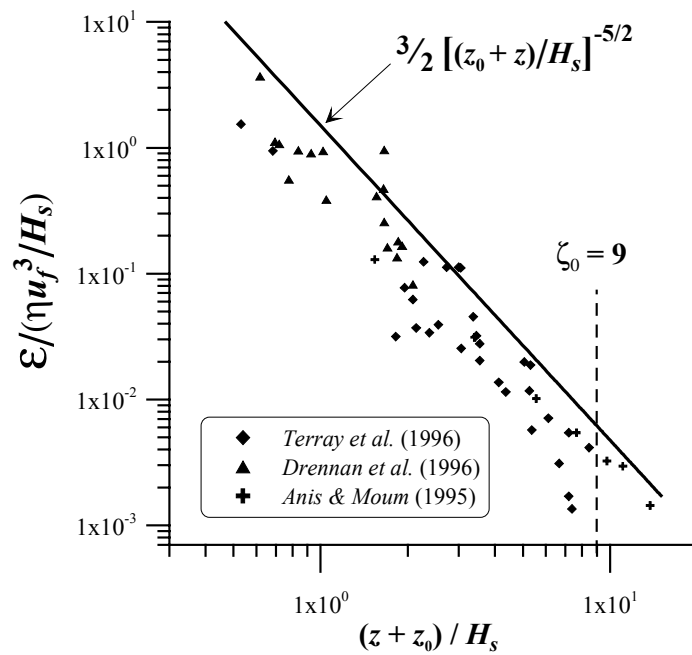


Figure 7-6: Analytical solution of the k - Ω system of primary turbulence variables for the wave-enhanced upper part of the epilimnion of deep large lakes.

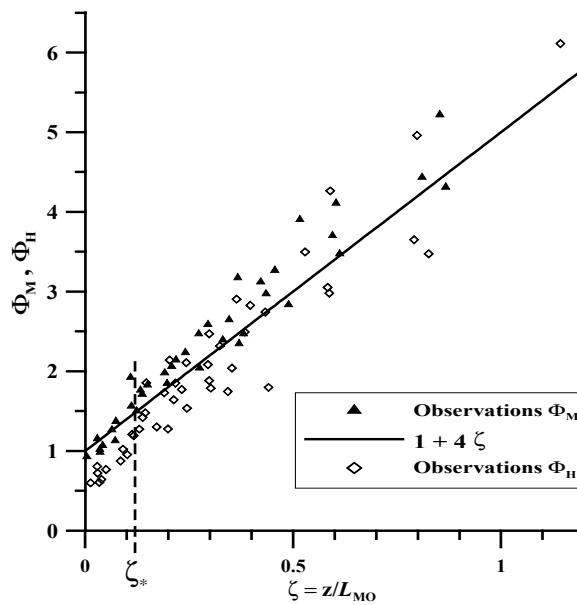


Figure 7-7: Analytical solution of the k - Ω system of primary turbulence for the Monin-Obukhov similarity problem in the upper part of the epilimnion of a lake. This solution holds for asymptotically large distances from the boundary for any system of primary variables. Close to the boundary it may only be understood if the action of shear-generated internal waves onto momentum and entrophy transport it taken into account.

7.3 APPLICATION TO LAKE GENEVA

Besides a numerical implementation of the closure presented above into the one-dimensional hydro-thermodynamic model LAKE-1D and its application to Lake Con-

stance and Loch Lomond in form of numerical long-term climate-change scenario simulations, the current closure may also be checked against the valuable observational data of the EUROLAKES partner EPFL.

In Figures 6-5 and 6-7 of this report, *Lemmin* from EPFL shows for Lake Geneva the following:

- The turbulent length scales L_T and L_O have about the same size and follow the rule $L_T \approx L_O \propto N^{-3/2}$.
- The eddy diffusivity, K_z [m^2s^{-1}], may be parameterized as follows: $K_z \approx 1.9 L_T^{4/3}$ (rounded values).

This behaviour may be explained by the present theory as follows.

The energy-containing length scale is $L = L_T/2$. For structural equilibrium we have $L/L_O = (2 R_g)^{3/4}$ such that $L_T = 2 L_O (2 R_g)^{3/4}$. By the definition of L_O , $L_O = \sqrt{\varepsilon/N^3}$.

For $R_g = \text{constant}$ and $\varepsilon = \text{constant}$ it follows directly the first of the above relations. For the data of the graph 6-5 we conclude $\varepsilon \approx O(10^{-10}) \text{ W kg}^{-1}$. Here we assumed full equilibrium, $R_g = 1/2$.

Now we consider the eddy diffusivity which in our terms is μ_t [$\text{m}^2 \text{s}^{-1}$]. In the above text we defined $\mu_t = \nu_t / \sigma$ where σ is the turbulent Prandtl number. In the fully stationary case it equals unity. Further, due to the Kolmogorov-Prandtl relation and the definition of the energy-containing length scale we have $\nu_t = \frac{1}{\pi^2} \frac{K_t^2}{\varepsilon} = \varepsilon^{1/3} L^{4/3}$. This relation nicely corresponds to the second scaling reported above by *Lemmin*; it is consistent with $\varepsilon \approx O(10^{-10}) \text{ W kg}^{-1}$.

7.4 CONCLUSIONS

The theoretical closure described above basically describes the internal mixing processes of deep large lakes like Lake Geneva fairly well in terms of analytical expressions and special solutions, as long as the dissipation rate, ε , does not vary too strongly. Basic assumptions which need to be used are

- the coexistence of turbulence and internal waves,
- the collapse hypothesis (slow turbulent motions are rapidly converted into wave motions if the time scale of turbulence is close enough to the Brunt-Väisälä period),
- the structural-equilibrium and
- the full-equilibrium statement.

The scatter of the data in the comparison between analytical scaling laws and observations as given in Figs. 6-5 and 6-7 may substantially be reduced if the corresponding meteorological forcing would be known and used to force a numerical implementation of the theoretical closure given above and outlined in much greater detail in Appendix A to this report. In this Appendix also the case of non-homogeneous shear layers is treated successfully. Here it is shown that the proper description of the fate of short internal waves, which radiate energy from the TKE pool away and which modify the standard turbulent momentum balance of the overall flow, still represent a challenge for future research. Related studies should preferably be carried out in deep large lakes where the experimental and observational access to the natural processes is much easier than in the ocean or coastal waters. Here the processes proceed with only minor influence from the margins or boundaries which would be the case of small and/or shallow lakes would be selected as study sites.

References

References not given here may be found in ANNEX A to this Final Report D25.

Baumert, H., and G. Radach, Hysteresis of turbulent kinetic energy in nonrotational tidal flows: A model study, *J. Geophys. Res.*, 97, 3669 - 3677, 1992.

Baumert, H., and H. Peters, Second-moment closures and length scales for weakly stratified turbulent shear flows, *J. Geophys. Res.*, 105, 6453 - 6468, 2000.

Baumert, H., and H. Peters, Turbulence closure, steady state, and collapse into waves. *J. Phys. Oceanogr.*, submitted 5 July 2002, 2003a.

Baumert, H., and H. Peters, A "natural" two-equation 3D turbulence closure. In preparation for submission to *J. Phys. Oceanogr.* 2003b.

Kleine, E. and H. Baumert, On an elementary interpretation of the Omega turbulence closure equation. In preparation for submission 2003.

Burchard, H. and H. Baumert, On the performance of a mixed-layer model based on the k- ϵ turbulence closure, *J. Geophys. Res.*, 100, 8523 - 8540, 1995.

Bournet PE. 1996. Contribution à l'étude hydrodynamique et thermique du Bourget Lake. PhD Thesis.

Dillon, T.M., 1982, Vertical overturns: a comparison of Thorpe and Ozmidov length scales. *J. Geophys. Res.*, 87, 9601-9613.

Gregg, M.C. 1994. Scaling turbulent dissipation in the thermocline. *J. Geophys. Res.*, 94, 9686-9698.

Garcon, V.C., Baumert, H., Schrimpf, W. and J.D. Woods (1993) - Fluctuations: a task package for the physicists. In: Towards a Model of Ocean Biogeochemical Processes (ed.: G.T. Evans und M.J.R. Fasham), *NATO ASI Series Vol. I* 10, 47 - 70, Springer-Verlag.

Henderson-Sellers B. 1987. Engineering Limnology. Pitman
Hodges B.R., Imberger J., Laval B., Appt J. Modelling the Hydrodynamics of Stratified Lakes. Hydroinformatics 2000.

Imberger, J. and G.N. Ivey, 1993. Boundary mixing in stratified reservoirs. *J. Fluid Mech.*, 248, 477-491.

Imberger, J. and G.N. Ivey, 1991. The nature of turbulence in a stratified fluid, part 2: application to lakes. *J. Phys. Oceanogr.*, 21, 659-680.

Imberger, J. and J.C. Patterson, 1990. Physical limnology. In: Advances in Applied Mechanics, *T. Wu (ed.)*, Academic Press, Boston, 27, 303-475.

Janin JM, Lepeintre F, and Pechon P. 1992. TELEMAC-3D: a finite element code to solve 3D free surface flows problems. Proceedings of computer modelling of seas and Coastal regions. Southampton, UK.

- Lemmin, U. 1998. Courantologie Lémanique. *Archs. Sci. Genève*, 51, 103-120.
- Lemmin, U., C. Perrinjaquet and W.H. Graf, 1987. Etude de la variation saisonniere des phénomènes de mélange dns l'hypolimnin du Léman. *Rapp. Comm. Int. prot. Eaux Léman contre pollut. (CIPEL)*, 85-95.
- Lemmin, U., C. Perrinjaquet and W.H. Graf, 1989. Etude de la variation saisonniere des phénomènes de mélange dns l'hypolimnin du Léman. *Rapp. Comm. Int. prot. Eaux Léman contre pollut. (CIPEL)*, 89-105.
- Pacanowski, R. C., and S. G. H. Philander, Parameterization of vertical mixing in numerical models of the tropical oceans, *J. Phys. Oceanogr.*, 11, 1443 - 1451, 1981.
- Stefan H. and Ford D.E. 1975. Temperature dynamics in dimictic lakes. *J. Hydraulics Div. ASCE*, 101, HY 1: 97-114.
- Thorpe, S.A., 1987, Current and temperature variability on the continental slope. *Phil. Trans. Roy. Soc. London*, A323, 471-517.
- Thorpe, S.A., 1977, Turbulence and mixing in a Scottish Loch. *Phil. Trans. Roy. Soc. London*, A286, 125-181.
- Wijesekera, H.W., T.M. Dillon and L. Padman, 1993. Some statistical and dynamical properties of turbulence in the oceanic pycnocline. *J. Geophys. Res.*, 98, 22665-22679.
- Zhang S., U. Lemmin and E. Hopfinger, 1994, The variability of vertical finescale temperature structures in Lake Geneva. *Fourth International Symposium on Stratified Flows. Grenoble, France.*
- Zhang S. and U. Lemmin, Dynamics of vertical mixing; overturning scales and energetics in Lake Geneva (*in preparation*).